

Facultad de Física
Pontificia Universidad Católica de Chile

Master's Thesis submitted to Physics Faculty at
Pontificia Universidad Católica de Chile, Santiago, Chile
for the degree of
Master of Science

submitted by
Valentina Ortiz Guzmán
born in Brussels, Belgium

2018

Medical Faculty Heidelberg
Ruprecht-Karls-University Heidelberg

Master's Thesis
"Clinical Medical Physics"

submitted by

Valentina Ortiz Guzmán

born in Brussels, Belgium

2018

A dynamic nonlinear coupled differential equations model of tumor
growth and response to radiotherapy

This Master's thesis has been composed by
Valentina Ortiz Guzmán
at Pontificia Universidad Católica de Chile (PUC)

under the supervision of
Prof. Araceli Gago, PhD
Prof. Ignacio Espinoza, PhD
Pontificia Universidad Católica de Chile (PUC)

and

Prof. Christian Karger, PhD
German Cancer Research Center (DKFZ)

A dynamic nonlinear coupled differential equations model of tumor growth and response to radiotherapy:

Mathematical modeling plays a key role in understanding and predicting tumor growth as well as in anticipating the effects of the different treatments available. It may help to improve radiotherapy outcome providing important insights into some biological mechanisms of cancer to be incorporated into the treatment planning routine. In this thesis, a non-spatial, continuous mathematical model to simulate tumor growth and response to radiotherapy was developed. It is based on nonlinear ordinary differential equations, which model the most relevant biological mechanisms. Simulations were performed to fit the model to experimental growth curves, as well as to study the tumor response to a radiotherapy treatment. The sensitivity of the model to the different parameters was also analyzed. An open-source interface, which allows to interactively study the impact of the different parameters in the tumor growth, was developed. The model developed reflects known tumor behaviors and agrees within uncertainties with experimental data of tumor growth and radiation response. The response to treatment was found to be significantly sensitive to the tumor composition at the moment of irradiation. This thesis provides a tool to increase the understanding of tumor behavior. Different ways to deep in the present study and to improve the model developed are proposed as future work.

Declaration:

I hereby certify, that I have composed the Master's Thesis independently, that no source materials or aids other than those mentioned have been used and that all citations have been declared appropriately.

Location, Date

Signature

Contents

1	Introduction	9
2	Theoretical framework	11
2.1	Tumor radiobiology	11
2.1.1	Tumor growth	11
2.1.2	Radiation damage	11
2.2	Linear-quadratic model and oxygen effect	12
2.3	Tumor control probability	14
2.4	The model in Lefebvre <i>et al.</i> (2016)	15
3	Methods and materials	16
3.1	Dynamic tumor Model	16
3.1.1	Modeling tumor growth	16
3.1.2	Modeling radiotherapy treatment	20
3.2	Tumor response quantification	22
3.3	Computational tools	22
3.3.1	Python interactive tool	23
3.4	Pre-clinical experimental data	23
3.5	Simulations	24
3.5.1	Growth curves fitting	25
3.5.2	Tumor response to a radiotherapy treatment	28
3.5.2.1	Evolution during and after a radiotherapy treatment	28
3.5.2.2	TCP with and without oxygen effect	28
3.5.3	Parametric sensitivity analysis	28
4	Results	30
4.1	Python interactive tool	30

4.2	Simulations	31
4.2.1	Growth curves fitting	31
4.2.2	Tumor response to a radiotherapy treatment	33
4.2.2.1	Evolution during and after a radiotherapy treatment . .	33
4.2.2.2	TCP with and without oxygen effect	34
4.2.3	Parametric sensitivity analysis	35
5	Discussion	42
5.1	The tumor model	42
5.1.1	Tumor composition: proportion of cancer and healthy cells	42
5.1.2	Doubling time	43
5.1.3	Cell density	44
5.2	Simulations	44
5.2.1	Growth curves fitting	44
5.2.2	Tumor response to a radiotherapy treatment	45
5.2.2.1	Evolution during and after a radiotherapy treatment . .	45
5.2.2.2	TCP with and without oxygen effect	46
5.2.3	Parametric sensitivity analysis	50
5.2.3.1	Cell density ρ	50
5.2.3.2	Healthy cells consumption rate η_2	51
5.2.3.3	Parameters with negligible impact	51
5.3	Limitations of this study	51
6	Conclusion	54
7	Future work	55
8	Bibliography	56
9	Appendix	62
9.1	Python interactive tool code	62
9.2	Matlab main codes	66
9.2.1	Tumor growth	66
9.2.2	Tumor response to radiotherapy	69
9.2.3	TCP simulation	73

1. Introduction

Cancer is one of the leading causes of morbidity and mortality around the world, with approximately 14 million new cases estimated in 2012. This number is expected to increase by about 70% over the next two decades [1]. However, due to the advances in technology, it is a disease that nowadays can be treated and cured in many cases. Radiotherapy has been one of the two most effective treatments, and it is estimated that more than half of all cancer patients are treated with radiotherapy during the course of their illness [2, 3].

Radiotherapy uses ionizing radiation to kill tumor cells by damaging their genetic material. Since in reality not only the malignant cells are killed but also the healthy tissue is affected by radiation, modern radiotherapy is today concentrated in improving all the technology involved in treatment delivery, in order to apply the therapeutically sufficient dose to the tumor volume while sparing the surrounding normal tissues. In this regard, one of the challenges is the incorporation of biological information into the treatment planning routine. For example, a clear and detailed understanding of tumor progression is required. In order to achieve this, mathematical modeling represents a promising tool to provide important insights into the biological mechanisms behind this complex disease.

Mathematical modeling plays a key role in understanding and predicting tumor growth as well as anticipating the effects of the different treatments available. It can be useful to check the consistency of some biological hypothesis or to identify which measurements are needed to test a particular theory. Mathematical models may be classified according to their scale or whether the spatial dimension is integrated or not. At the microscopic scale, cells are tracked and usually considered individually by discrete modeling [4, 5, 6]. At macroscopic scales, continuum modeling is often used, where the evolution of densities or volume fractions describes tumor behavior [7, 8, 9]. According to the spatial dimension classification, non-spatial models, usually employing ordinary differential equations (ODEs), consider the overall status of some tumor features (such as volume, mass or radius) versus time [10, 11]. On the other hand, spatial models consider the spatial distribution of some internal tumor characteristics and their

evolution in time. Usually partial differential equations (PDEs) are used for that, such as reaction-diffusion equations. (Principles from continuum mechanics are also sometimes considered [9, 12]).

The objective of this study is to develop a non-spatial, continuous mathematical model based on nonlinear ordinary differential equations to simulate tumor growth and response to radiotherapy, considering certain biological mechanisms involved in tumor evolution. It must be able to reproduce tumor behavior, fitting measured growth and response curves data. As part of the goals, a study of parametric sensitivity is performed in order to identify which parameters of the model have greater impact on the simulated tumor growth and response. The final intention is to create a tool for simulating tumor behavior, during radiotherapy, using previously known experimental data of tumor growth together with some radiobiological parameter values. In the future, this may allow simulating the outcome of different treatment strategies and increasing the understanding on tumor behavior for the developing of personalized treatment planning.

Following this introduction, chapter 2 contains the theoretical framework used in this thesis. Then, a description of the methods and materials, with the details about the implementation of all simulations performed, is given in chapter 3. The main results are presented in chapter 4 and the corresponding discussion is addressed in chapter 5. Finally, chapter 6 presents a brief conclusion of this work, and the future work proposed is given in chapter 7.

2. Theoretical framework

2.1 Tumor radiobiology

2.1.1 Tumor growth

A tumor is an abnormal growth of tissue possessing no physiological function that arises from rapid and uncontrolled cellular proliferation due to genetic mutations [13]. This unrestrained growth implies a metabolic demand that rapidly exceeds the diffusion limit of oxygen and nutrients, reason why the tumor needs to develop its own nutrient supply in order to continue growing [14, 15]. Thus, two stages in the growth of a tumor can be distinguished: initial avascular growth and subsequent vascular growth, which in turn may induce metastatic spread [12]. During the second phase, new vasculature is formed from the pre-existing blood vessels by a process known as angiogenesis, which starts with the production of VEGF (vascular endothelial growth factors), a signal protein, released by cancer cells in this case, that travels to nearby vessels and induces vascular growth. Nevertheless, the new vasculature is functionally abnormal, very primitive and chaotic in nature. Furthermore, this process lags behind the faster tumor growth. As a result, new vessels are unable to meet the requirements on oxygen and nutrients of the rapidly expanding tumor mass, leading to the appearance of hypoxic areas in the tumor [14, 15].

From a macroscopic point of view, the tumor growth curve (i.e., volume versus time) has a shape characterized by two defined stages: an initial exponential portion related to rapid tumor growth, followed by a saturation zone of reduced growth [16, 17]. Exponential growth is possible when enough availability of nutrients and oxygen is present (during the initial avascular growth). Later, because of a lower availability of nutrients and oxygen, the growth becomes slower (saturation zone during vascular growth).

2.1.2 Radiation damage

Ionizing radiation (IR), as its name evokes, is a type of radiation carrying on enough energy to ionize (liberate electrons from) atoms and molecules within matter. When

ionizing radiation is absorbed in biological material, cell damage may occur in one of two ways: direct or indirect. Direct damage is caused when radiation interacts directly with the deoxyribonucleic acid (DNA) molecule, critical target of the cell. Atoms are ionized or excited, leading to a chain of events that eventually produce biological damage [18]. Indirect damage is caused by free radicals produced when radiation interacts with other molecules (mainly water) within the cell. These molecules are highly reactive and produce a cascade of chemical changes leading to the disruption of the DNA structure, which may also conclude with irreversible biological damage.

Because of the random nature of energy deposition by IR, any component of the cell may be damaged, but most of them are present in multiple copies and therefore damaging a few does not have great repercussions. Instead, DNA is present in only two copies and encodes information required to synthesize proteins and regulate many cellular functions. Therefore, when it is damaged the cell viability is endangered. However, cells have developed a series of efficient repair processes to withstand this harm. This is the reason why, in spite of the approximately 10^5 ionizations produced in one cell by 1 Gy (1Gy=1 J/Kg) of radiation dose, resulting in more than 2000 lesions to the DNA, only approximately the 30% of the cells are killed in such an event [14]. Cells that cannot repair their DNA die, or lose their ability to generate colonies. Dead cells are reabsorbed by macrophages through a process called phagocytosis.

2.2 Linear-quadratic model and oxygen effect

The Linear-Quadratic (LQ) model quantifies the survival of cells exposed to IR. According to this model, the survival fraction SF of cells irradiated with a single dose d is expressed as: [18]

$$SF = e^{-(\alpha d + \beta d^2)} \quad (2.1)$$

This model assumes that there are two components to cell kill by radiation, represented by the linear and quadratic terms. The parameter α describes the unreparable (lethal) cell damage. The parameter β describes the repairable (sub-lethal) damage that, accumulated, eventually produces death.

It is known that the response of cells to IR is strongly dependent on the oxygen availability, being the hypoxic cells more resistant [14]. This can be explained by the "oxygen fixation hypothesis" [19]: when radiation is absorbed in a biological material, free radicals R^\bullet are produced within the cell (e.g., in water or/and DNA). These free radicals may break chemical bounds and initiate the chain of processes that leads to biological damage. The radicals produced in the critical target (DNA) are unstable molecules and will react rapidly with oxygen to produce another radical, finally resulting in a stable change in the chemical composition of the target. This damage is said to be "fixed" and is more difficult to repair. If no oxygen is present, R^\bullet molecules have a longer half-life and can react with H^+ , thus chemically restoring its original form. In this case, no damage occurs [14].

The dependence of radiation damage with oxygen can be quantified through a parameter called the oxygen enhancement ratio (OER). The OER is defined as the ratio between the dose required to produce a certain biological effect in hypoxic conditions and the dose required to produce the same effect in oxic conditions (or under the actual oxygen concentration) [18]:

$$OER = \frac{D(\text{hypoxic})}{D(\text{oxic})} \Bigg|_{\text{same biological effect}} \quad (2.2)$$

Therefore, an OER value of 3 means that hypoxic cells need 3 times more dose than oxic cells to get the same biological effect. When the oxygen effect is not considered, the LQ-model could lead to cell killing overestimation (or survival fraction underestimation). One way to overcome this issue is to incorporate the oxygen dependence in the cell killing expression. The OER has been quantified as [20]:

$$OER(P_{O_2}) = \frac{OER_m \cdot P_{O_2} + K_m}{P_{O_2} + K_m} \quad (2.3)$$

where OER_m is the maximum OER value, P_{O_2} is the oxygen partial pressure, and K_m is the oxygen partial pressure at which $OER = (OER_m + 1)/2$. Then, the surviving fraction can be determined by:

$$SF = e^{-\left(\frac{\alpha}{OER_m} d \cdot OER(P_{O_2}) + \frac{\beta}{OER_m^2} d^2 \cdot OER^2(P_{O_2})\right)} \quad (2.4)$$

where α and β refer to oxic conditions.

2.3 Tumor control probability

One of the relevant endpoints in radiotherapy is the Tumor Control Probability (TCP), which is the probability that a given dose of radiation will lead to tumor control. "Tumor control" means that all the clonogenic tumor cells (cells that are able to proliferate and form new tumors) are either killed or have lost their ability to produce colonies. TCP versus dose is a dose-response relationship represented by a sigmoid curve (see Figure 2.1). The probability of control tends to zero at very low doses and tends to 1 at very large doses. This continuous shape, in contrast to a sudden discontinuity between 0 and 1, can be explained by the radiosensitivity variability in a population of patients and from the random nature of cell killing. Although there are several functions with the properties mentioned, the following logistic formulation is commonly used [14]:

$$TCP(D) = \frac{1}{1 + e^{-b_0 - b_1 D}} \quad (2.5)$$

where D is the total dose and b_0 and b_1 are fitting parameters.

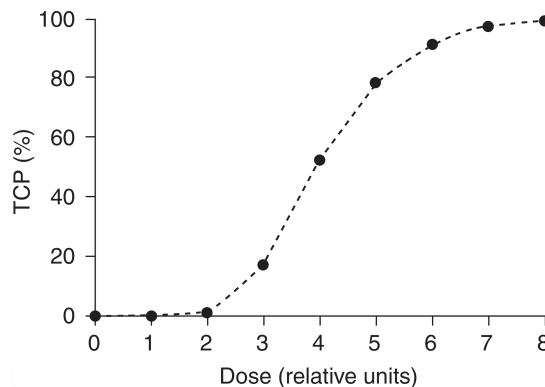


Figure 2.1: Example of a TCP curve, where the probability of tumor control is given in percentage [14].

TCP curves are commonly used to quantify the response to treatment instead of tumor volume evolution with dose, because of temporal inflammation processes occurring in tumors during and after irradiation. This implies that in many tissues, the tumor volume increases during the course of the treatment despite the reduction of the number of living tumor cells.

2.4 The model in Lefebvre *et al.* (2016)

A brief description of a previous study on tumor modeling, on which the present model is based, is given here. For details see the reference cited. In [9] a spatial model was built, using the observations from medical images (CT scans), for modeling growth and resistance to drug therapies of liver gastrointestinal stromal tumor metastases. The model parameters values were estimated through comparison with clinical data from the images, for which a numerical reconstitution of the CT scans was developed. After this calibration, the model reproduced qualitatively and quantitatively the spatial tumor evolution of one specific patient.

This spatial model developed consists in a set of non-linear partial differential equations (PDEs). The tumor is described through densities of proliferative cancer cells and necrotic cells. Healthy cells are also included to model the healthy tissue surrounding the tumor. Cell density variations are driven by transport equations. Vascularization and nutrients supply are taken into account with the introduction of only one variable that describes both, since nutrients are supplied to the tumor by the vascularization. The evolution of this quantity is described with a diffusion equation. The effect of growth factors on vascularization is also considered through another variable, standing for the mean concentration of endothelial growth factors (EGF) produced by cancer cells. This quantity modulates the amount of nutrients/vascularization through an integro-differential equation. The rates of cell proliferation and (natural) death due to lack of nutrients depend on the amount of nutrients available, through regularized Heaviside functions.

3. Methods and materials

3.1 Dynamic tumor Model

In the following sections, the mathematical model of tumor growth and response to radiotherapy developed in this work is presented. This model, consisting on a group of coupled ordinary differential equations, takes into account the biological mechanisms involved in tumor evolution like: nutrient-dependent tumor growth leading to initial exponential growth and subsequent Gompertzian-like slower growth, hypoxia induced tumor vascularization driven by tumor angiogenesis, which depends on endothelial growth factors concentration, cell death due to lack of nutrients, radiation-induced cell killing with an indirect simulation of the oxygen effect and reabsorption of dead cells. The modeling of tumor growth, based on a previous work by Lefebvre *et al.* [9], is described in section 3.1.1. Section 3.1.2 describes the modeling of the radiotherapy treatment and the corresponding tumor response.

3.1.1 Modeling tumor growth

The growth of a tumor is described by the following five ordinary differential equations for the proliferative (tumor) cells, P , healthy cells, H , necrotic cells, N , vascularization providing nutrients and oxygen, M , and endothelial growth factors (EGF), ξ :

$$\frac{dP}{dt} = (\gamma_{pp}(M) - \gamma_{pd}(M))P \quad (3.1)$$

$$\frac{dH}{dt} = (\gamma_{hp}(M) - \gamma_{hd}(M))H \quad (3.2)$$

$$\frac{dN}{dt} = \gamma_{pd}(M)P + \gamma_{hd}(M)H - \delta(\epsilon_\delta + M)N \quad (3.3)$$

$$\frac{dM}{dt} = C_0 H \left(1 - \frac{M}{2M_{th}}\right) - \eta_p(M)P - \eta_h(M)H + C_1 \xi \quad (3.4)$$

$$\frac{d\xi}{dt} = aP(\epsilon_\xi - \gamma_{pp}(M)/\gamma_{0p}) - \lambda\xi \quad (3.5)$$

The main difference from the reference study (by Lefebvre *et al.*) is that the present model does not consider a spatial description, therefore ordinary differential equations instead of partial differential equations are used. Cells and nutrient transport, arising from reaction or diffusion are not present here. Equations (3.1)-(3.3) have the same form of their corresponding from [9], except that they do not include the terms related to death due to drug treatments. Equation (3.4), compared to its counterpart from [9], also includes terms associated to the consumption of nutrients/oxygen by the healthy cells and the dependency of the vascularization with the EGF (last two terms of (3.4)). Again, in equation (3.5), spatial related terms are not included, neither terms related with the drug treatment, as done in [9].

The quantities γ_{pp} and γ_{pd} correspond to the proliferation and death rate functions, respectively, for the tumor cells P . γ_{hp} and γ_{hd} are the corresponding proliferating and death rates for the healthy cells H . These rates depend on the availability of nutrients (M) in the form:

$$\gamma_{pp}(M) = \begin{cases} 0 & M \leq 0 \\ \gamma_{0p} \frac{1+\tanh(R(M-M_{th}))}{2} & M > 0 \end{cases} \quad (3.6)$$

$$\gamma_{pd}(M) = \gamma_1 \max(0, -\tanh(R(M - M_{th}))) \quad (3.7)$$

$$\gamma_{hp}(M) = \begin{cases} 0 & M \leq 0 \\ \gamma_{0h} \frac{1+\tanh(R(M-M_{th}))}{2} \left(1 - \frac{H}{H_0}\right) & M > 0 \end{cases} \quad (3.8)$$

$$\gamma_{hd}(M) = C_h \gamma_1 \max(0, -\tanh(R(M - M_{th}))) \quad (3.9)$$

where it is established that in absence of M no proliferation is possible, and natural cell death occurs only when M is lower than a reference value M_{th} , which corresponds to the hypoxia/nutrients starvation threshold. Equations (3.6) and (3.9) are the same as in [9]. The tumor cell death rate, γ_{pd} , was defined here in the same form of healthy cell death rate, instead of having the same form of γ_{pp} , as it is done in [9]. While no proliferation rate of healthy cells is considered in [9], in the present model it is defined through equation (3.8). This function is similar to the proliferation rate of tumor cells, but includes a term to reflect the homeostasis property of the healthy tissue. There is proliferation only while $H < H_0$, where H_0 is the initial number of healthy cells.

The nutrient consumption is described by $\eta_p(M)$ for P cells and $\eta_h(M)$ for H cells. Unlike [9], where these rates are constant, the present model defines consumption rates as functions of M , given by:

$$\eta_p(M) = \begin{cases} 0 & M \leq 0 \\ \eta_1 \tanh\left(\frac{M}{M_{th}}\right) & M > 0 \end{cases} \quad (3.10)$$

$$\eta_h(M) = \begin{cases} 0 & M \leq 0 \\ \eta_2 \tanh\left(\frac{M}{M_{th}}\right) & M > 0 \end{cases} \quad (3.11)$$

These dependencies were inspired by the fact that the oxygen consumption rate remains practically constant for high oxygen levels and decreases (rapidly) as the oxygen concentration decreases [21].

Most of the parameters involved in the previous equations are related with biological mechanisms: γ_{0p} and γ_{0h} are the maximum proliferation rates, i.e the ones for well

oxygenated conditions, for tumor and healthy cells, respectively; γ_1 is the maximum apoptosis rate for tumor cells and C_h is the ratio of healthy to tumor cells maximum apoptosis rates; δ is the elimination rate of necrotic cells and ϵ_δ is a parameter ensuring the elimination process still occur in case M is equal to zero; C_0 is the angiogenic capacity rate of the healthy tissue; η_1 and η_2 are the maximum rates of nutrient consumption by tumor and healthy cells, respectively; C_1 accounts for the dependency of the vascularization with the EGF; a is the angiogenic excitability rate; ϵ_ξ stands for the ground production of growth factors by cancer cells and λ is the elimination rate of angiogenic growth factor signal. Finally, R is a numerical parameter for regulating the steepness of the hyperbolic tangent function. Consequently, this parameter allows to modulate the softness of the regularized Heaviside functions that drive the rates of cell proliferation and cell death (equations (3.6)-(3.9)).

The parameter δ , associated with death cells reabsorption, is defined through the equation:

$$\delta(\epsilon_\delta + Mth) = \frac{\ln(2)}{7} \quad (3.12)$$

which establishes that the amount of necrotic cells is reduced by a factor of 2 in a period of time of approximately seven days [6]. This model assumes that this occurs at $M = M_{th}$.

The growth rate of tumor cells γ_{0p} is defined through the doubling time DT_p , which is the time required for the tumor cells to double its volume, as:

$$\gamma_{0p} = \frac{\ln(2)}{DT_p}. \quad (3.13)$$

The tumor volume is the sum of the three existing type of cells divided by the cell density, ρ , which is assumed to be equal among the different cell types and remains constant throughout time. Therefore, tumor evolution is driven by the dependence on time of the quantity $P + H + N$. Then, the tumor volume V is calculated as:

$$V = \frac{P + H + N}{\rho}. \quad (3.14)$$

All the parameters used to model tumor growth are summarized in Table 3.1.

The equations (3.1)-(3.5) govern the tumor growth before radiotherapy treatment and between treatment fractions of irradiation.

Table 3.1: List of the parameters of the model with their meaning and units (d=day).

Parameter	Meaning	Unit
DT_p	Doubling time of tumor cells	d
γ_{0h}	Growth rate of healthy cells	1/d
γ_1	Apoptosis rate of tumor cells	1/d
C_h	Ratio of healthy cells to tumor cells apoptosis rate	
R	Smoothing parameter	-
M_{th}	Hypoxia threshold	-
C_0	Angiogenic capacity rate of healthy tissue	1/d
C_1	Dependence of vascularization with the EGF rate	1/d
η_1	Consumption rate of tumor cells	1/d
η_2	Consumption rate of healthy cells	1/d
λ	Elimination rate of angiogenic growth factor signal	1/d
a	Angiogenic excitability rate	1/d
ϵ_ξ	Ground production of EGF	-
ϵ_δ	Ground elimination rate of necrotic cells	-
ρ	Cell density	cells/cm ³

3.1.2 Modeling radiotherapy treatment

This model considers that radiotherapy is delivered instantaneously. This is adequate for the high dose rates usually achieved in external radiotherapy and assumes that damage repair does not occur during irradiation [14]. Fractionated treatments are simulated using a fraction size of 2 Gy (this value might be easily changed to other values). Irradiation takes place once a day, 5 days a week, with no irradiation during weekends. Cell death due to irradiation is modeled as a stochastic process in the following way:

- (i) Just before a treatment fraction is delivered, the amount of tumor and healthy cells is computed.
- (ii) The survival probability for each cell type (tumor and healthy) is calculated.
- (iii) A stochastic cell kill is applied: a random number between 0 and 1 is sorted for

each cell (tumor and healthy). If this number is lower than the probability previously calculated, this cell remains alive. Otherwise, it dies due to the current treatment fraction delivered.

- (iv) The number of surviving cells is computed and used to update the initial conditions of the tumor ODE system, which is solved from this instant until the time corresponding to the next fraction.

The survival probability (S) is given by the LQ model described in section 2.2:

$$S = \exp \left[-\alpha_{eff}(OER) \left(d + \frac{d^2}{(\alpha/\beta)_{eff}(OER)} \right) \right] \quad (3.15)$$

where α_{eff} and $(\alpha/\beta)_{eff}$ correspond to the effective values of α and α/β , respectively. These values depend on the oxygen enhancement ratio, as they do in equation (2.4), in the form:

$$\alpha_{eff}(OER) = \frac{\alpha}{OER_m} OER \quad (3.16)$$

$$(\alpha/\beta)_{eff}(OER) = \frac{\alpha/\beta}{OER} OER_m \quad (3.17)$$

The OER has the same form as in equation (2.3), but replacing P_{O_2} by M :

$$OER(M) = \frac{M \cdot OER_m + K_m}{M + K_m} \quad (3.18)$$

The parameter K_m was fixed as a function of the hypoxia threshold and the maximum value of the OER :

$$K_m = M_{th}(OER_m - 2) . \quad (3.19)$$

The parameters α and α/β have different values for tumor and healthy cells (different radiosensitivity), consequently the survival probability S will be different for each type of tissue. The radiosensitivity of tumor cells was taken to be 3 times larger than the radiosensitivity of healthy cells, based on previous studies [22].

3.2 Tumor response quantification

Tumor response is quantified through TCP curves. To generate a TCP curve, the response of the virtual tumor to radiotherapy is simulated several times and at different dose levels. To include interpatient radiosensitivity variations, each one of the n simulations at each dose level is performed with a different α value. This value is sampled from a Gaussian distribution, with a mean (intrinsic) α value and a standard deviation equal to 15% of the mean, as done in previous studies [23, 24]. At each dose level, the fraction of controlled tumors is determined, being the TCP value for that dose. TCP curves are fitted to the logistic TCP model (equation 2.5), using the bootstrapping method to quantify the associated uncertainties [25]. The tumor control dose 50%, TCD_{50} (defined as the dose at which 50% of tumor control probability is reached), is calculated as:

$$\text{TCD}_{50} = \frac{-b_0}{b_1}. \quad (3.20)$$

3.3 Computational tools

All the codes for modeling the tumor growth and treatment response, were written and solved in MATLAB R2016b and R2017a (The Mathworks Inc., MA). Additionally, the tumor growth model was also implemented in Python language (Python 3.6.3 version) using Jupyter Notebook [26], an open-source web application that allows to create and share documents containing codes. This code was used to change interactively some values of the parameters of the tumor growth model and visualize the effect. Section 3.3.1 provides a brief description of this program. The main codes (Matlab and Python) developed in this study are shown in the Appendix (Section 9).

3.3.1 Python interactive tool

This tool allows to perform parametric sensitivity studies instantaneously, showing the impact of certain parameter values variations in the evolution of the tumor model. This is achieved through the manipulation of slider buttons. For each parameter there is a slider button, which one can move according to a range of values previously defined. Together with the panel of all parameter sliders, the plots of the quantities of interest are displayed. The curve of the evolution with time of any quantity can be shown (P , H , N , V , etc.). The change of the curve due to parameters values variation is visualized while moving the corresponding slider.

3.4 Pre-clinical experimental data

Pre-clinical experimental data of tumor growth and response to radiotherapy treatment were used for the studies performed in this thesis. In order to fit the model to experimental growth data, four human head and neck squamous cell carcinoma (HNSCC) tumor growth curves (from three different cell lines) were considered: OSC19 and HN5 lines from [27], FaDu line from [28], and FaDu line from Bothwell *et al.* [29]. The response to treatment was compared with experimental dose response data taken from Yaromina *et al.* [30]. Since the FaDu tumor cell line was used for all the analyses performed in this study (growth fitting, treatment response and parametric sensitivity), only the reference studies corresponding to this tumor cell line are described in this section.

Bothwell *et al.* (2016) [29]: In this work, the preclinical effect of vascular disrupting agents (VDAs) was investigated using *in vivo* models of human HNSCC of the FaDu tumor cell line. A subcutaneous xenograft model was established by the inoculation of 1×10^6 FaDu cells into the flank of mice. Tumor volume measurements were performed to assess tumor response to VDA therapy. The curve corresponding to the control group was used for comparison with the tumor growth model developed in this thesis.

Yaromina *et al.* (2011) [30]: In this work, microenvironmental parameters during frac-

tionated irradiation in human HNSCC xenografts were studied. Tumor pieces (~ 1 mm in diameter) of six different tumor cell lines were transplanted subcutaneously into nude mice. Depending on the tumor type, 30 to 160 Gy total doses were given in 30 fractions within 6 weeks. Among others, local tumor control probabilities due to radiotherapy were determined. TCP curves were calculated and radiation response was quantified as the dose required to control 50% of tumors (TCD_{50}). Data corresponding to the FaDu tumor cell line was considered for comparison with the responses simulated in the present study because its response is intermediate, not too sensitive neither too resistant. Additionally, information about the tumor volume achieved since transplantation (V_y) (until treatment) and the mean value of the elapsed time between tumor transplantation and the beginning of the treatment (t_y), were also considered as a reference to the model.

3.5 Simulations

Simulations performed in this study aimed to check if the tumor model reproduces the behavior of real tumors. Additionally, the impact of the different parameters on tumor growth and response was also studied. Regarding tumor growth, the reproduction of the growth curves (volume versus time) shape and the development of hypoxia were investigated. Regarding treatment response, the level of oxygenation and the oxygen dependent response behavior were analyzed. Adjustments of the model to experimental curves/data were performed in order to obtain the parameter values that allow to reproduce these real scenarios.

The simulations performed can be divided in:

1. simulation of tumor growth, used to fit the parameters of the model to experimental growth data, and get the corresponding parameters values,
2. simulation of radiotherapy treatment and tumor radiation response (as TCP curves) with and without oxygen effect, and
3. parametric sensitivity analysis of the model through the inspection of tumor growth and TCP curves over a range of values for each parameter.

Details about how simulations were implemented are presented in the next subsections. The model parameters affecting tumor growth (those in equations (3.1)-(3.11)) were varied in order to fit the model to experimental data. The parameters involved in the response to radiation, namely the ones related with cells radiosensitivity, were fixed to values taken from the literature, and are shown in Table 3.2.

Table 3.2: Biological parameters of treatment response used for the simulations.

Parameter		Value
Maximum value of the OER	OER_m	2.5 [20, 31]
Radiosensitivity of tumor cells (LQ model)	α_p	0.41 Gy ⁻¹ [32, 33]
	$(\alpha/\beta)_p$	10 Gy [34]
Radiosensitivity of healthy cells (LQ model)	α_h	0.13 Gy ⁻¹ [22]
	$(\alpha/\beta)_h$	4.4 Gy [35]

Two different proportions of tumor and healthy cells composing the initial tumor were investigated. First, the tumor is assumed to be composed by 90% tumor cells and 10% healthy cells (case A). Second, a composition of 10% tumor cells and 90% healthy cells, was considered (case B). This was done in view of the variable information available regarding tumor composition. A tumor is known to be composed of tumor cells, part of them called stem cells, and stroma (which include normal cells), but the amount of each one is not clearly established (see Section 5.1.1 for a major discussion). Some previous studies consider only tumor cells (although different kinds of them) for modeling tumor growth [10, 36]. Other models include normal cells in the simulation of tumor growth [5, 6].

3.5.1 Growth curves fitting

The methodology followed to fit the model of tumor growth to the experimental growth curves available (OSC19, HN5 & FaDu) was similar in all cases. Since the FaDu tumor cell line was also used to evaluate the model of response to radiation, details about the fitting of this tumor growth curve will be presented here.

To fit the experimental FaDu growth curve from Bothwell *et al.* [29], the simulation is performed starting from the first point of the experimental curve (volume versus time). The two proportions of tumor and healthy cells assumed led to two different sets of parameters values, A1 and B1, that fit this experimental curve. To fit the experimental growth data from Yaromina *et al.* [30], which consists only in the initial tumor volume implanted and the tumor volume just before the beginning of the treatment (t_y, V_y) , the two proportion cases were also considered, leading to sets A2 and B2, respectively. For the other HNSCC lines (OSC19, HN5, FaDu from [28]), only case A was considered.

For the determination of both A1 and B1 sets of parameters, the initial condition on tumor size was first set according to the value derived from the experimental curve from [29] ($\sim 77.12 \text{ mm}^3$ tumor volume). Then, the following procedure was carried out: some parameters values, such as those standing for the doubling time (DT_p), cell density (ρ) and rate of necrotic cells elimination (δ), were established within ranges according to information found in the literature [15, 36, 37, 38]; for other parameters, preliminary values based on the model by Lefebvre *et al.* [9] were chosen; the remaining parameters were set performing a manual preliminary adjustment to the experimental growth curve, using the Python interactive interface for evaluating tumor evolution. Then, a fit of the model to the experimental growth curve was performed, based on least squares differences minimization. For this, the manually adjusted parameter values were used as first guess.

Parameter values from sets A1 and B1 were used as a reference to define sets A2 and B2, that fit the experimental data point (t_y, V_y) for the FaDu tumor cell line from Yaromina *et al.* [30], used to study the response to radiotherapy. First, the initial condition on the tumor size was changed to fulfill the one described in [30] (a tumor volume of $\sim 0.52 \text{ mm}^3$, corresponding to $\sim 1 \text{ mm}$ of diameter). The two different proportions of tumor and healthy cells were again considered. Then, starting from the values of sets A1 and B1, certain parameters were readjusted (see Table 4.1 from Section 4), using the Python interactive tool, in order to fit the point (t_y, V_y) . This led to A2 and B2 sets of parameter values, respectively. The meaning of the labels for all sets above-mentioned is summarized in Table 3.3.

Table 3.3: Summary of the labels used for the sets of parameters.

Label	Proportion case
A	90% tumor cells, 10% healthy cells
B	10% tumor cells, 90% healthy cells
Label	Experimental data
1	Bothwell <i>et al.</i> [29]
2	Yaromina <i>et al.</i> [30]

The initial conditions used to solve the PDE system in all the tumor growth simulations were established according to the information found in the corresponding publication. These conditions are specified in Table 3.4. For the case of the OSC19 and HN5 tumor cell lines, the number of cancer cells inoculated is given [27]. This number was used as the initial number of tumor cells (P_0) and an initial tumor composition of 90% tumor cells and 10% healthy cells was considered to define the initial number of healthy cells (H_0) (rows 2 and 3 of Table 3.4). For the case of FaDu growth curves, the information available is the initial tumor volume, therefore the initial number of tumor and healthy cells is affected by the value of the cell density parameter (ρ). Additionally, these values depend on the proportion of tumor and healthy cells considered. The initial conditions for the necrotic cells (N), nutrients/oxygen (M), and endothelial growth factors (ξ) were the same for all lines simulated: $N_0 = 0$, $M_0 = 4$, $\xi_0 = 2$.

Table 3.4: Initial conditions used for the simulations. For OSC19 and HN5 lines (upper rows), the quantities P_0 and H_0 are shown separately. For FaDu line (bottom row), the total number of initial cells $P_0 + H_0$ is given, since the individual values for P_0 and H_0 depend on the proportion of tumor and healthy cells (A or B) considered. FaDu from Altogen Laboratory [28] (left), FaDu from Bothwell *et al.* [29] (middle) and FaDu from Yaromina *et al.* [30] (right).

	OSC19 [27]	HN5 [27]	
P_0	1×10^5 cells	2×10^5 cells	
H_0	1.1×10^4 cells	2.2×10^4 cells	
	FaDu [28]	FaDu [29]	FaDu [30]
$P_0 + H_0$	$77.12 \cdot \rho$ cells	$67.77 \cdot \rho$ cells	$0.52 \cdot \rho$ cells

3.5.2 Tumor response to a radiotherapy treatment

3.5.2.1 Evolution during and after a radiotherapy treatment

The response of the virtual tumor to radiotherapy treatment was checked for sets A2 and B2. A treatment of 30 fractions of 2 Gy in 6 weeks, starting at day 24 from the beginning of the growth (as in [30]), was simulated. All evolution curves, including tumor volume, nutrients/oxygen, tumor cells and healthy cells, were stored.

3.5.2.2 TCP with and without oxygen effect

Treatment response was simulated using the parameter values from sets A2 and B2. The response of these two virtual tumors was then compared to the response data from [30]. Moreover, the influence of oxygen in the response of the virtual tumors was studied by performing simulations with and without considering the oxygen effect. Here, “with oxygen effect” refers to the dependence of the radiosensitivity parameters, α and α/β , with oxygen (through the OER), as is established in the model through equations (3.15)-(3.18). “Without oxygen effect” means that this dependence is omitted, therefore keeping these values as constants and recovering the original LQ expression for the survival fraction (equation (2.1)). It is worth to mention that the effect of oxygen in other mechanisms such as proliferation or cell death due to lack of nutrients/oxygen was considered in the two simulations. Values of TCD_{50} were calculated from the simulated TCP curves.

3.5.3 Parametric sensitivity analysis

In order to analyze the sensitivity of the model to the different parameters and identify which affect more importantly growth and response, a general parametric sensitivity study was performed. For each parameter, three different values (initial, minimum and maximum) were used to calculate growth and response curves while maintaining all the other parameters values fixed. Set A2 was used as the reference for this analysis. The initial (‘init’) values correspond to the ones achieved in the fitting to the experimental curve (see Table 4.1, Section 4). The selection of the minimum (‘min’) and maximum (‘max’) values was done according to the following: the interactive Python

tool was used to evaluate whether a certain parameter importantly modified the growth curve, meaning that its variation effect was visible. For those parameters whose variation sensibly affects the growth, the minimum and maximum values were chosen in such a way that the growth curve fit the experimental point $(t_y, V_y) \pm 10\%$ of the tumor volume (in the ordinate axis). In other words, the parameter values that make the tumor growth curve pass through the point $(t_y, V_y + 0.1V_y)$ and through the point $(t_y, V_y - 0.1V_y)$ were defined as the extremes (minimum or maximum) values. For those parameters whose variation seems to have almost no effect in the growth curve, the minimum and maximum values were selected as 1/10 and 10 times the initial value, respectively. In addition to these criteria, for some parameters, the range of variation was constrained to values found in the literature (for DT_p and ρ). The parameter γ_{0h} , on the other hand, was also constrained to not exceed the maximum value of γ_{0p} (given by the minimum DT_p value). It is worth noting that in some cases the parameter turned out to be hybrid, in the sense that the variation in one direction significantly modified the growth curve but not in the other direction.

4. Results

4.1 Python interactive tool

The tumor growth model was implemented in Python, as an interactive tool, in order to visualize the relative importance of the different parameters on the tumor growth. A screenshot of the interface developed for this interactive analysis of the tumor model is shown in Figure 4.1. Additionally, a working example code of the Python interactive tool can be found in the Appendix (Section 9).

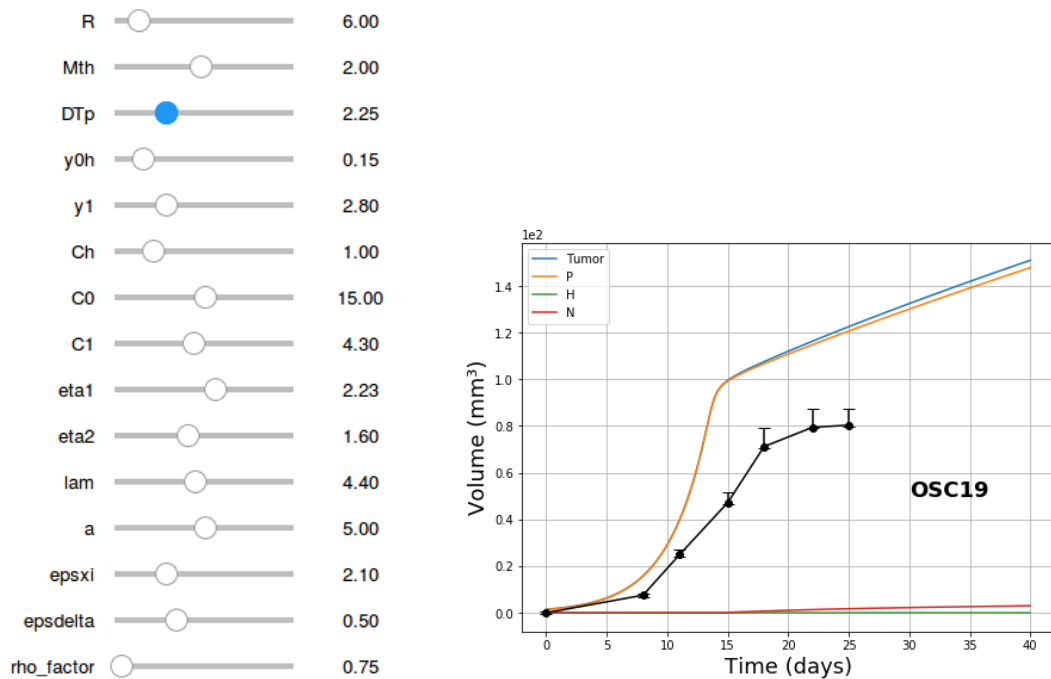


Figure 4.1: Screenshot of the interface coded in Python, using Jupyter Notebook, developed for evaluating tumor growth interactively. The example shows the experimental growth curve (black points and line), with error bars, of the OSC19 tumor cell line from [27].

4.2 Simulations

4.2.1 Growth curves fitting

Figure 4.2 shows the simulated growth curves (tumor volume versus time) adjusted to the experimental growth curves. Black dots with error bar correspond to the experimental data and blue solid lines correspond to the simulated virtual tumor.

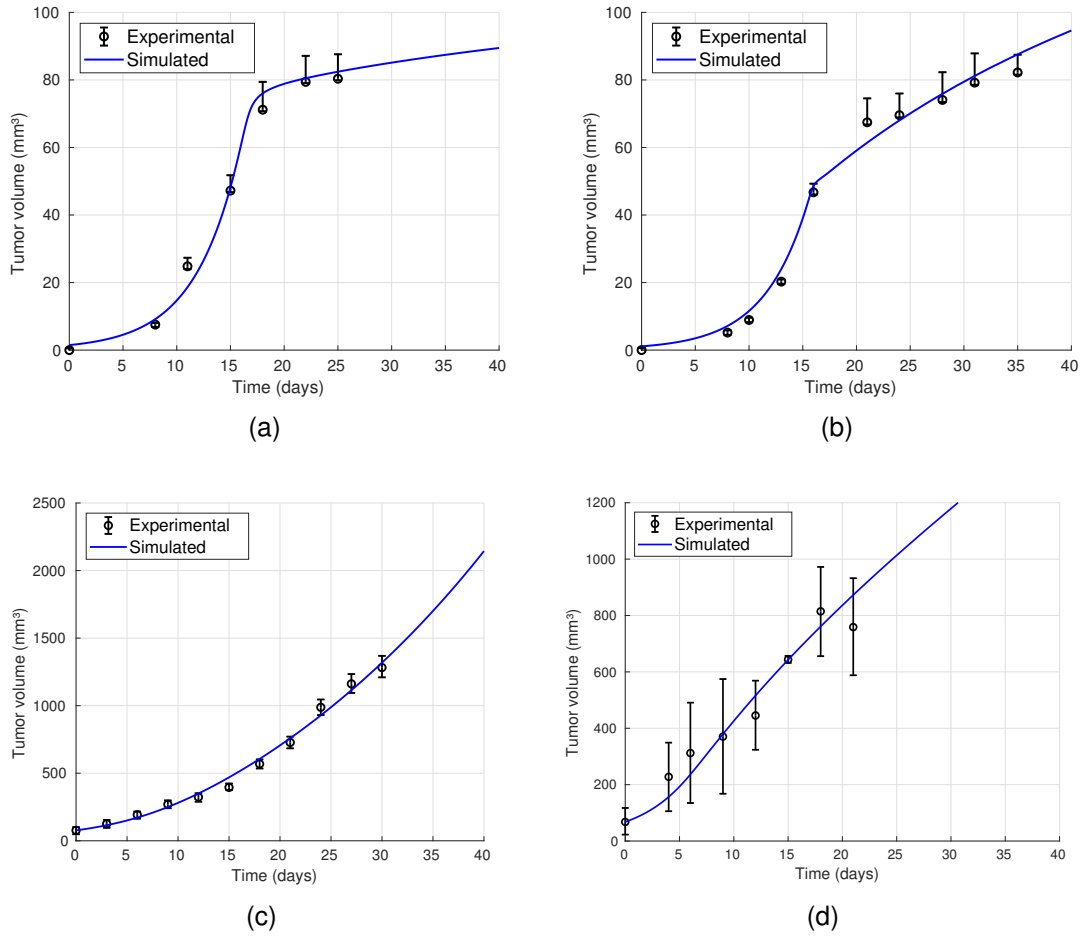


Figure 4.2: Fit of the model to the experimental growth curves of three tumor cell lines: (a) OSC19 [27], (b) HN5 [27], (c) FaDu from Altogen Labs [28], and (d) FaDu from Bothwell *et al.* [29]. Simulations performed with case A of tumor composition (90% of tumor cells and 10% of healthy cells at $t=0$ days).

Parameter values of sets A1, B1, A2 and B2, which fit the experimental data of the FaDu tumor cell line from Bothwell *et al.* [29] and Yaromina *et al.* [30], are shown in Table 4.1. Figure 4.3 shows the tumor growth curves simulated with sets A1 and B1. Figure 4.4 shows the tumor growth curves simulated with sets A2 and B2 to fit the volume achieved in the study of Yaromina *et al.* at day 24.

Table 4.1: Parameters values used for the simulations. Set A1 and B1 fit the experimental data from [29]. Sets A2 and B2 fit the experimental data from [30]. Refer to Table 3.1 for the corresponding units. Last two rows show the initial conditions (considering the value of the cell density ρ and the proportion case) used for each case.

Parameter	A1	B1	A2	B2
DT_p	3.07	1.2	1.4	1.2
γ_{0h}	0.20	0.20	0.20	0.20
γ_1	5.0e-3	5.0e-3	5.0e-3	5.0e-3
C_h	1.0	1.0	1.0	1.0
R	2.4	2.4	2.4	2.4
M_{th}	2.0	2.0	2.0	2.0
C_0	6.61e-06	1.20e-06	6.61e-06	9.0e-06
C_1	4.62e-2	2.30e-2	4.62e-2	4.22e-2
η_1	1.96e-07	1.95e-07	1.96e-07	1.95e-07
η_2	1.7e-07	1.55e-07	1.7e-07	1.55e-07
λ	4.69	4.48	4.69	4.48
a	3.11e-06	2.48e-06	3.11e-06	3.16e-06
ϵ_ξ	2.71	2.71	3.17	2.71
ϵ_δ	0.7	0.7	0.7	0.7
ρ	1e8	1e8	1e8	1e8
P_0	6.1×10^6 cells	6.8×10^5 cells	4.7×10^4 cells	5.2×10^3 cells
H_0	6.8×10^5 cells	6.1×10^6	5.2×10^3 cells	4.7×10^4 cells

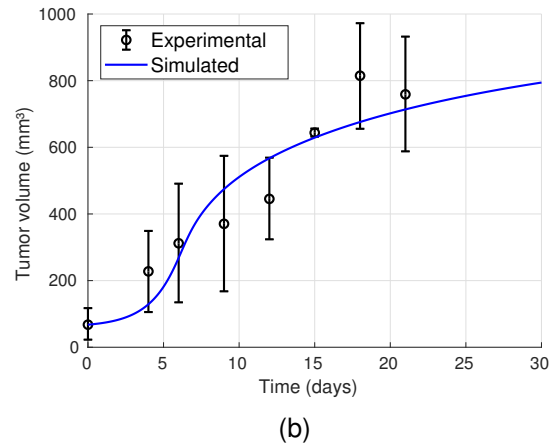
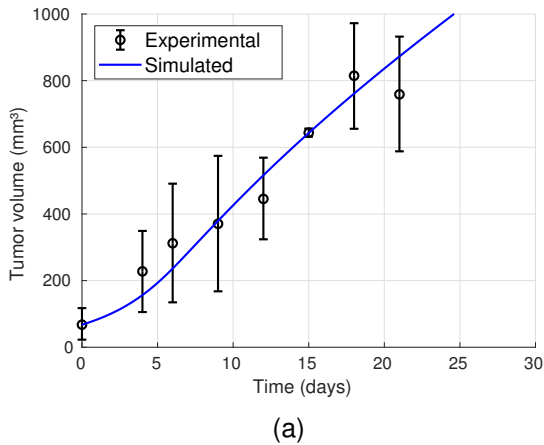


Figure 4.3: Fit of the model to the experimental growth curve (black points, with error bars) of FaDu tumor cell line from Bothwell *et al.* [29], with the two proportions of tumor and healthy cells considered. (a) Set A1. (b) Set B1.

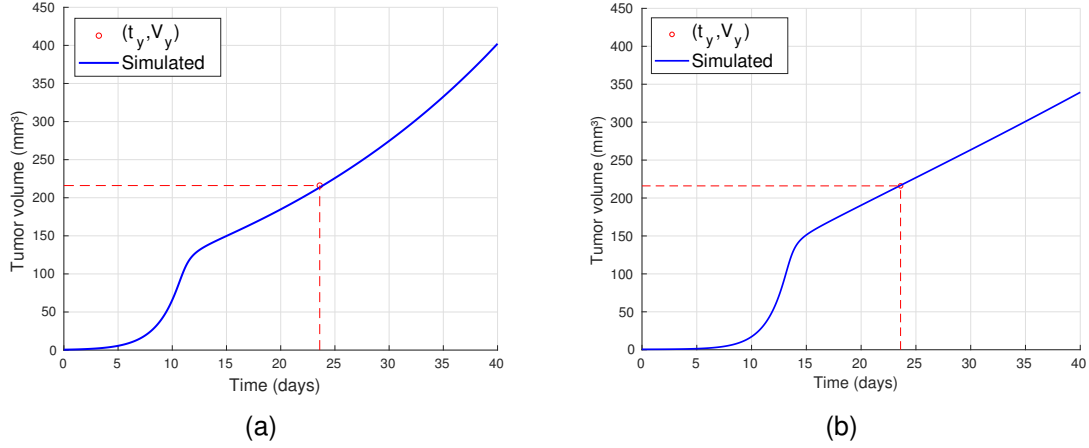


Figure 4.4: Tumor growth curves for FaDu cells simulated with (a) set A2 and (b) set B2. Red dashed lines indicate the position of the experimental data point (t_y, V_y) from Yaromina *et al.* [30].

4.2.2 Tumor response to a radiotherapy treatment

4.2.2.1 Evolution during and after a radiotherapy treatment

The evolution of the virtual tumors (A2 and B2) during a radiotherapy treatment of 30 fractions of 2 Gy is shown in Figure 4.5. For both sets it is observed that when the treatment starts, tumor and healthy cells decrease rapidly. After irradiation has ceased, the population of healthy cells increases again. Tumor cells also regrow if, at least, one tumor cell remains alive at the end of the treatment (which is the case in these simulations).

Regarding tumor composition, as already mentioned, two different proportion of tumor and healthy cells were considered for the tumor initial condition (yielding to sets A2 and B2). However, at the moment in which treatment begins, this proportion was changed due to the tumor growth. At day 24, when the treatment starts, the tumor was composed mainly for tumor cells (more than 99%) for both sets. Healthy cells, on the other hand, were found to be in a proportion of approximately 0.02% in set A2, and 0.2% in set B2.

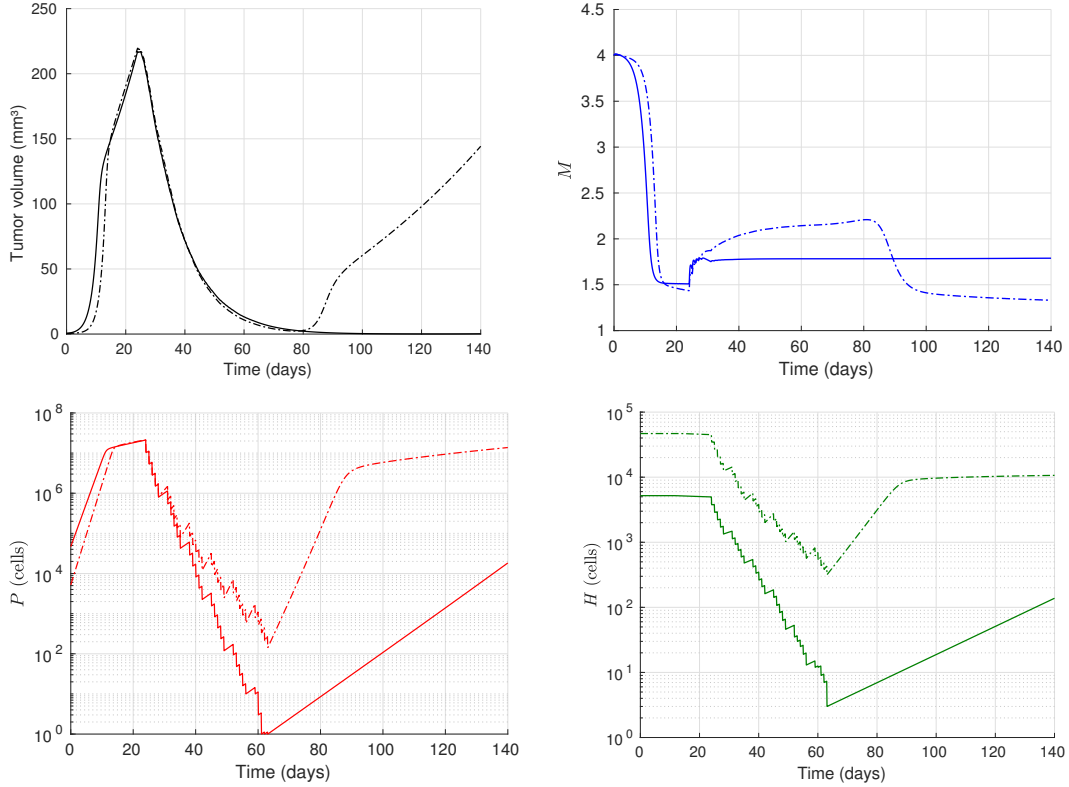


Figure 4.5: Evolution of relevant tumor quantities with radiotherapy treatment simulated with set A2 (solid line) and set B2 (dash-dotted line). Tumor volume (upper left), nutrients/oxygen supply (upper right), tumor cells in logarithmic scale (bottom left), and healthy cells in logarithmic scale (bottom right).

4.2.2.2 TCP with and without oxygen effect

Figure 4.6 shows the TCP curves calculated with and without oxygen effect on tumor sensitivity to radiation, for the two sets simulated. Values of dose required to control 50% of tumors (TCD_{50}) are presented in the figure. Red curves correspond to the case in which the oxygen radiosensitivity dependence is taken into account to simulate the response. Black curves represent the cases for which oxygen effect was not considered. It can be seen that these curves are shifted to the left with respect the red ones by 15.45 Gy for set A2, and by 41.21 Gy for set B2. The TCD_{50} value reported by Yaromina *et al.* [30] was 61.5 Gy, with an uncertainty range of 56-68 Gy. This is also shown in Figure 4.6.

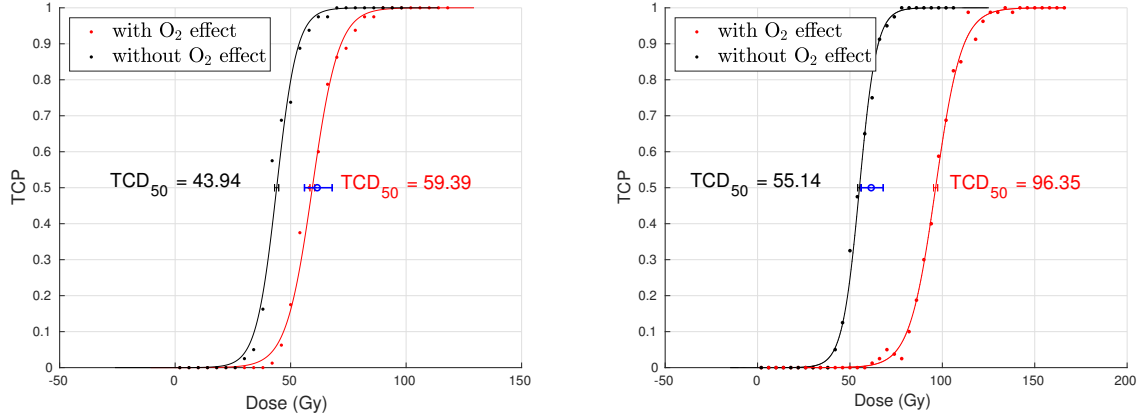


Figure 4.6: Simulated TCP curves (points), and logistic fitting (lines), with oxygen effect (red) and without oxygen effect (black), for set A2 (left) and set B2 (right). The TCD_{50} value reported in [30], with its corresponding uncertainty, is also shown (blue circle and horizontal bar).

4.2.3 Parametric sensitivity analysis

Figures 4.7-4.21 show simulated tumor growth curves (without treatment) and TCP curves calculated with each parameter value. Black solid lines correspond to the initial parameter value, blue dashed lines to the minimum value, and red dotted ones to the maximum value. The three parameter values are shown in the figure. TCD_{50} values resulting for those parameter values are also presented in the charts.

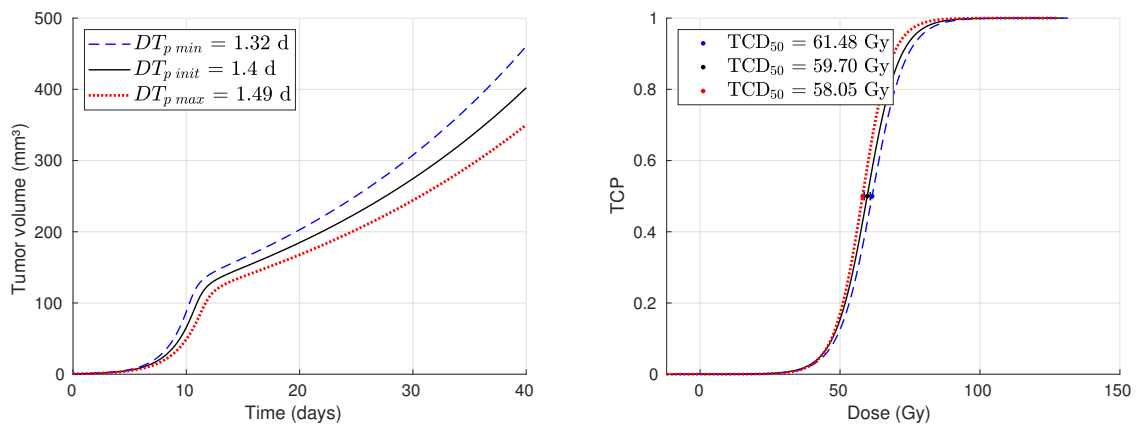


Figure 4.7: Simulated tumor growth curves (left) and dose-response curves (right), for the three different values of the parameter DT_p .

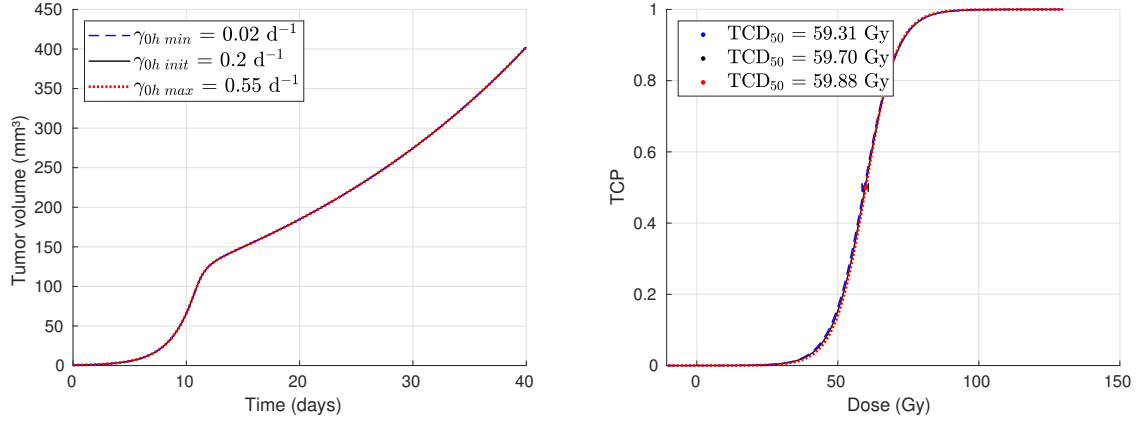


Figure 4.8: Simulated tumor growth curves (left) and dose-response curves (right), for the three different values of the parameter γ_{0h} .

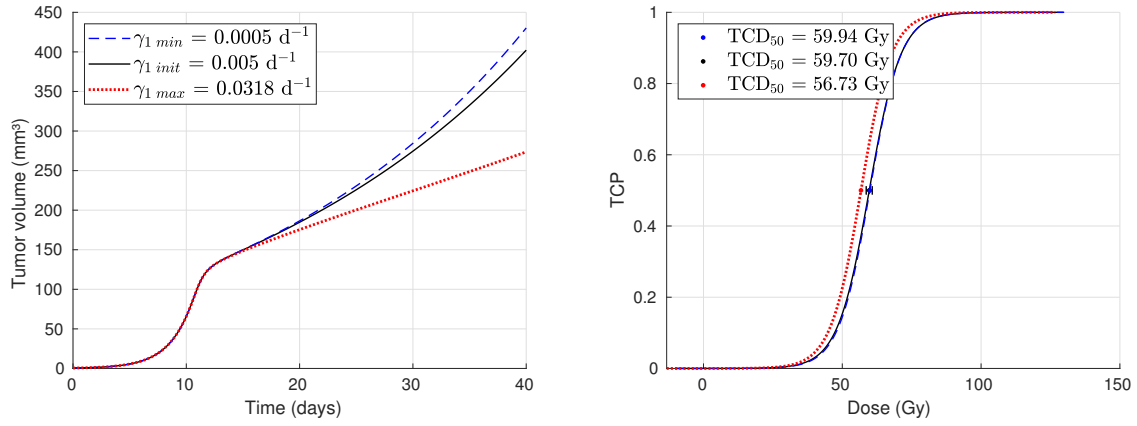


Figure 4.9: Simulated tumor growth curves (left) and dose-response curves (right), for the three different values of the parameter γ_1 .

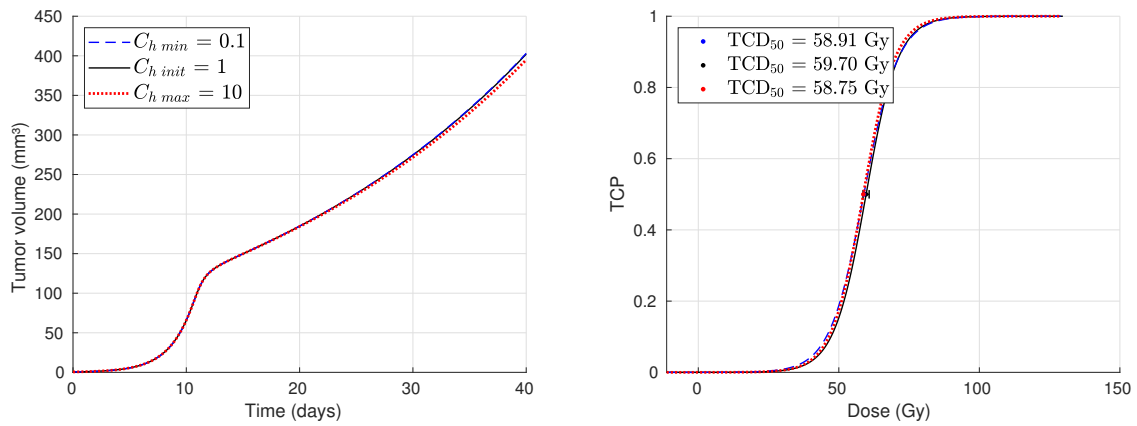


Figure 4.10: Simulated tumor growth curves (left) and dose-response curves (right), for the three different values of the parameter C_h .

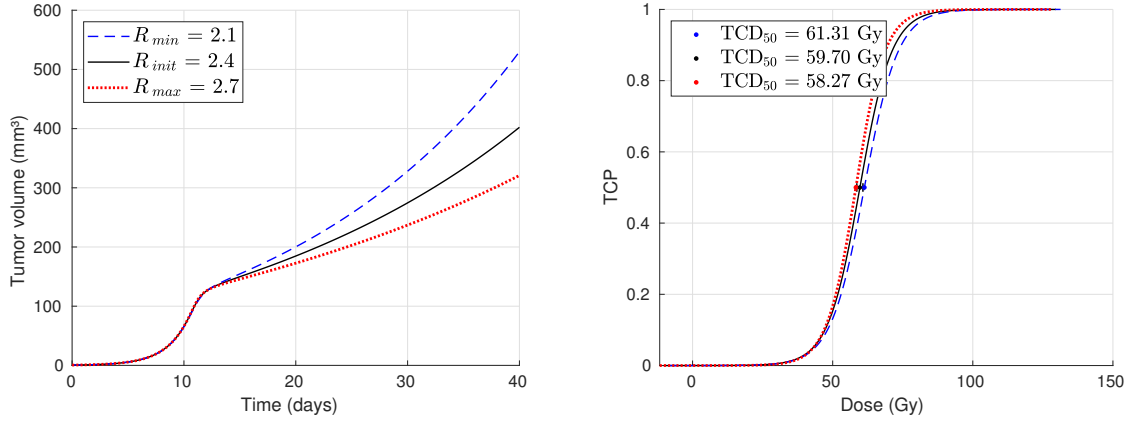


Figure 4.11: Simulated tumor growth curves (left) and dose-response curves (right), for the three different values of the parameter R .

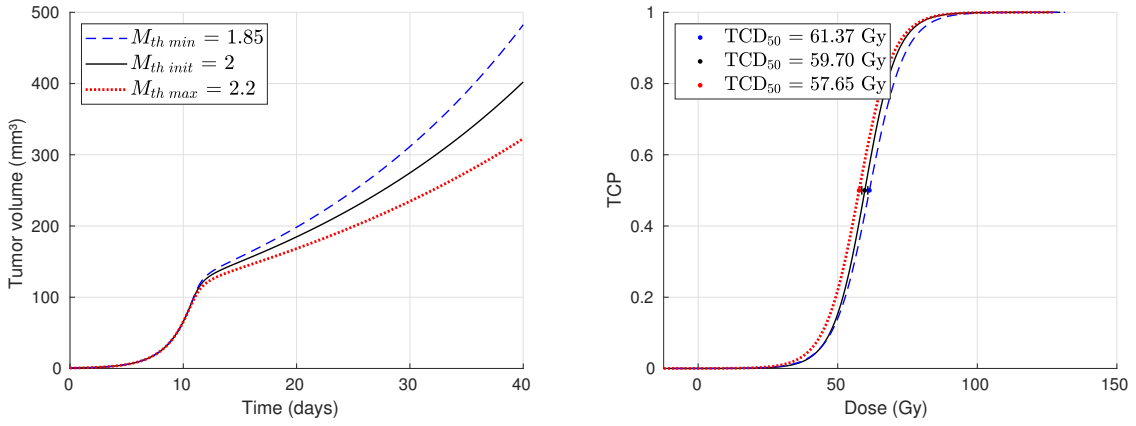


Figure 4.12: Simulated tumor growth curves (left) and dose-response curves (right), for the three different values of the parameter M_{th} .

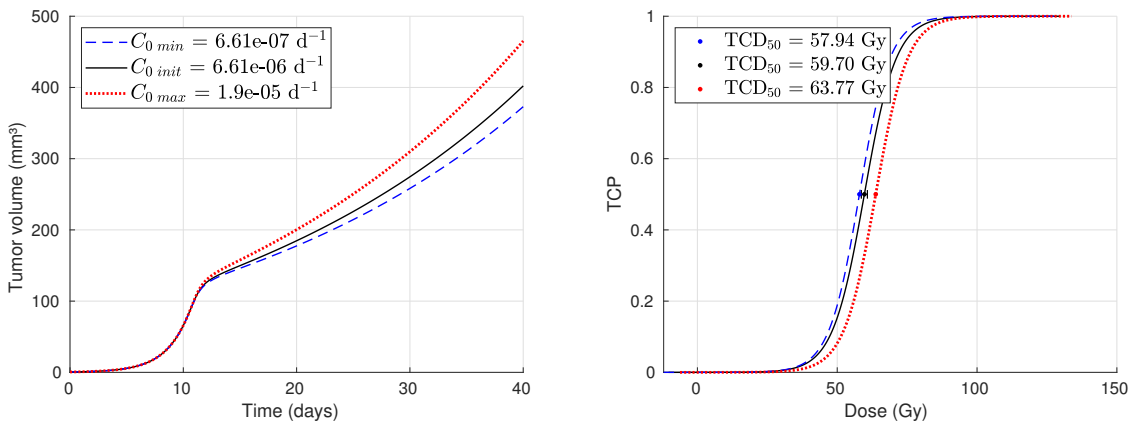


Figure 4.13: Simulated tumor growth curves (left) and dose-response curves (right), for the three different values of the parameter C_0 .

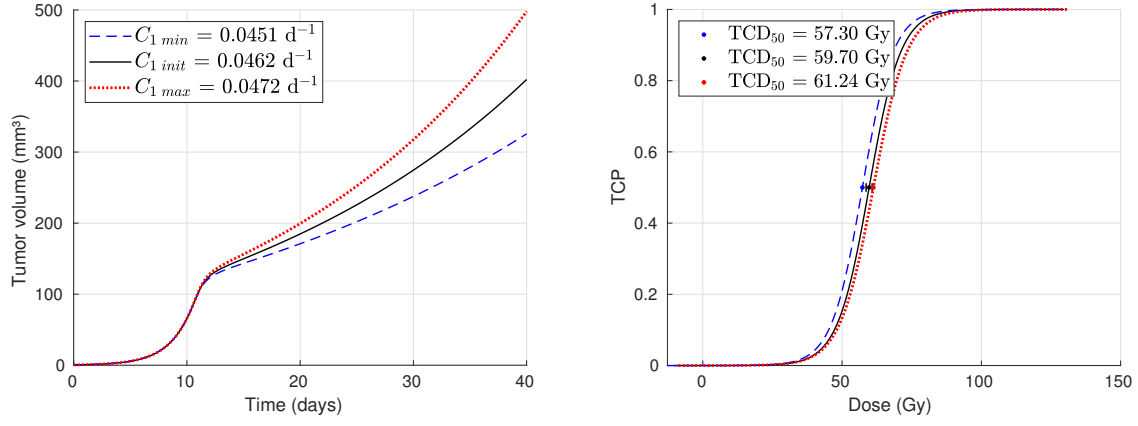


Figure 4.14: Simulated tumor growth curves (left) and dose-response curves (right), for the three different values of the parameter C_1 .

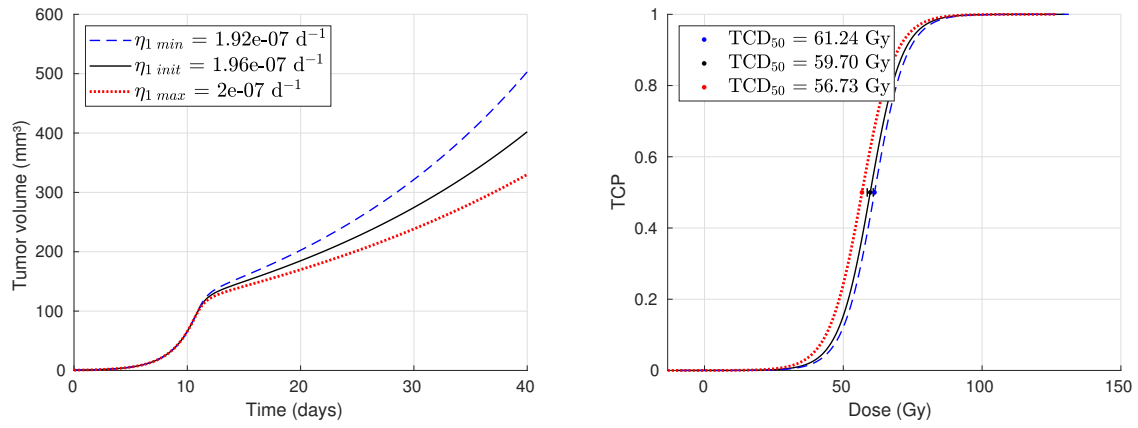


Figure 4.15: Simulated tumor growth curves (left) and dose-response curves (right), for the three different values of the parameter η_1 .

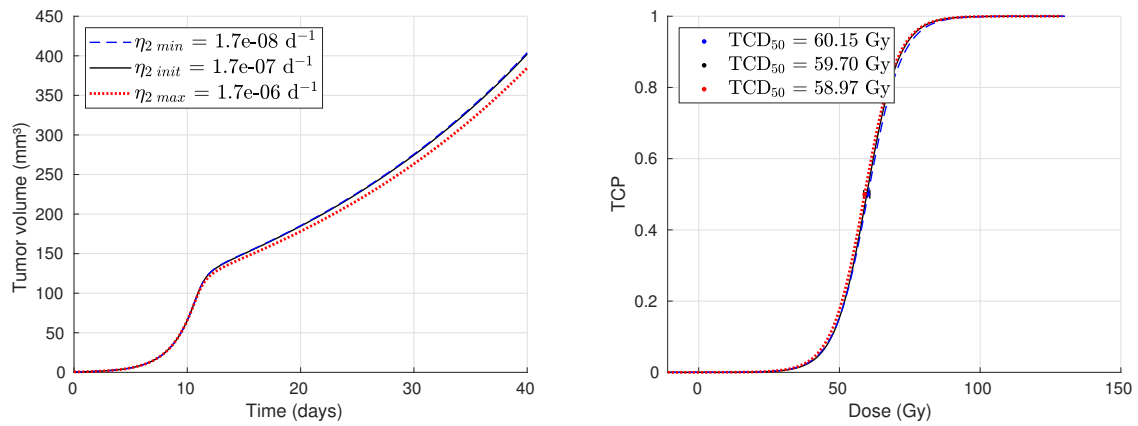


Figure 4.16: Simulated tumor growth curves (left) and dose-response curves (right), for the three different values of the parameter η_2 .

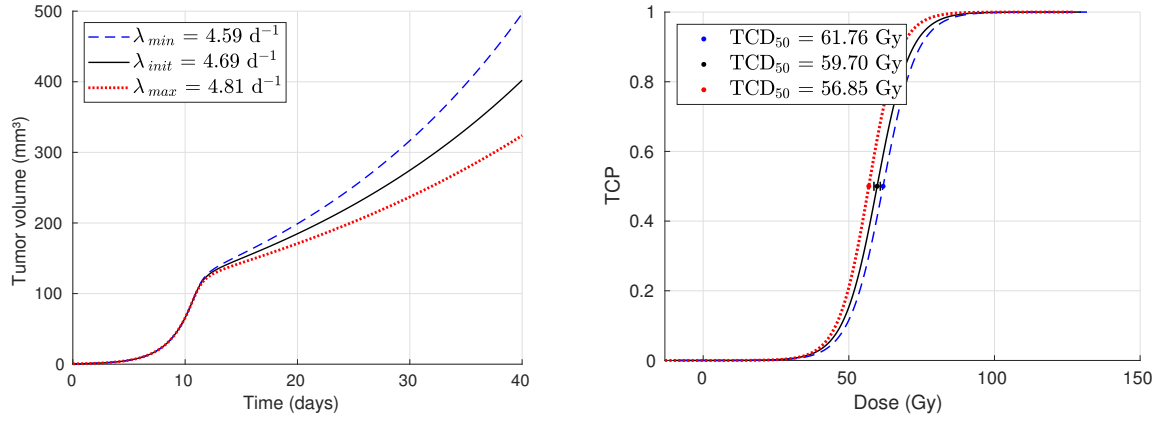


Figure 4.17: Simulated tumor growth curves (left) and dose-response curves (right), for the three different values of the parameter λ .

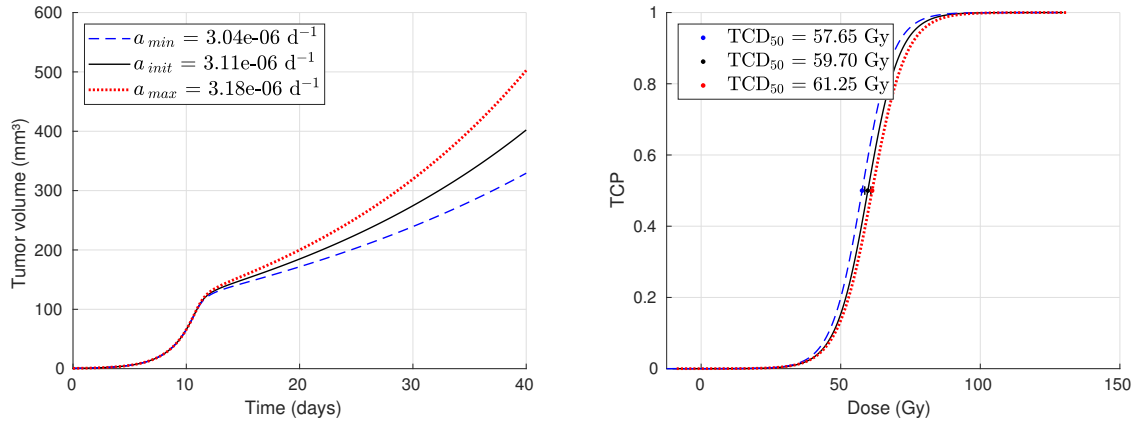


Figure 4.18: Simulated tumor growth curves (left) and dose-response curves (right), for the three different values of the parameter α .

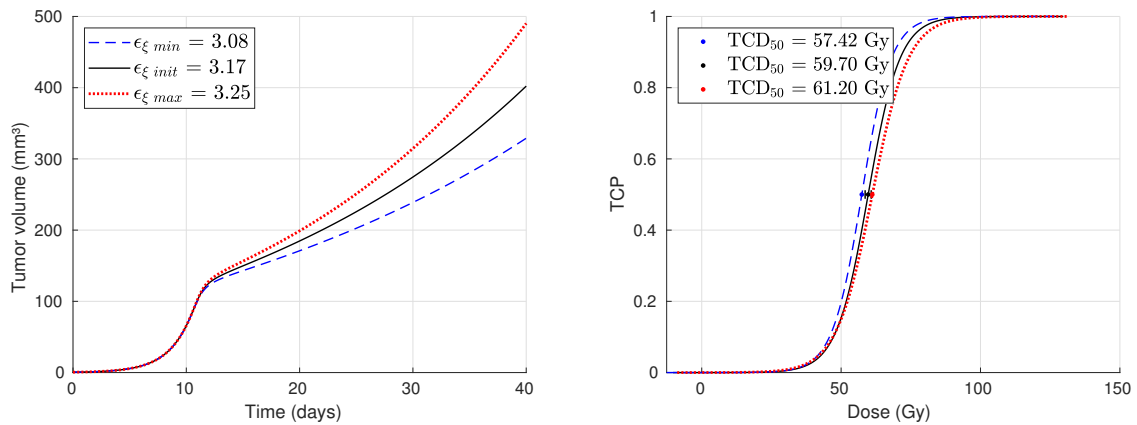


Figure 4.19: Simulated tumor growth curves (left) and dose-response curves (right), for the three different values of the parameter ϵ_{ξ} .

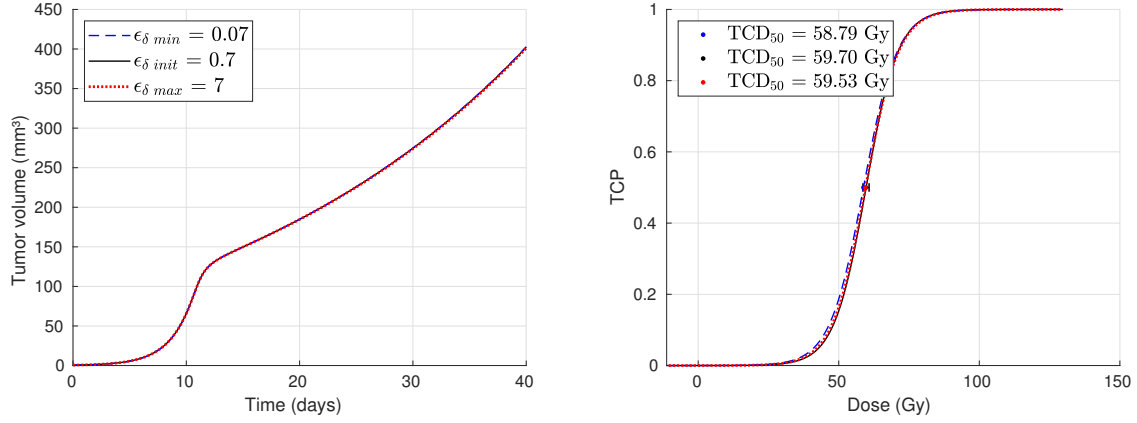


Figure 4.20: Simulated tumor growth curves (left) and dose-response curves (right), for the three different values of the parameter ϵ_δ .

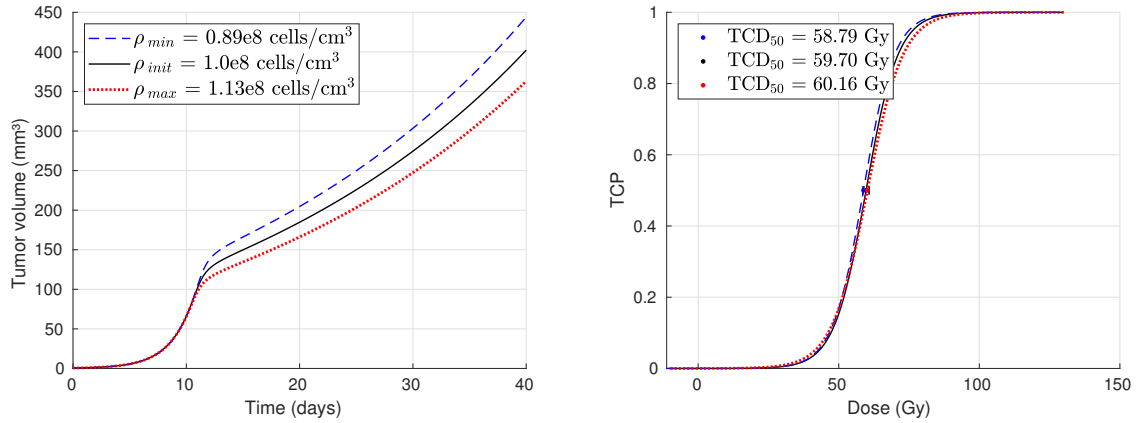


Figure 4.21: Simulated tumor growth curves (left) and dose-response curves (right), for the three different values of the parameter ρ .

These figures show how the different parameters affect the growth and the response of the tumor. The higher the values of the angiogenic capacity rate, C_0 , angiogenic excitability rate, a , dependence of nutrients/oxygen (vascularization) with EGF rate, C_1 , and ground production of growth factors, ϵ_ξ , the faster the tumor growth (leading to larger tumors) and consequently higher TCD_{50} values were observed. On the other hand, higher values of tumor cells doubling time DT_p , smoothing parameter R , tumor cell death rate, γ_1 , hypoxia threshold, M_{th} , nutrient consumption by tumor cells, η_1 , and elimination rate of angiogenic growth factor signal, λ , led to slower growth and therefore response curves are shifted towards lower doses. For the healthy cells, variation of nutrients/oxygen consumption rate, η_2 , is observed to produce a small difference in tumor growth, but almost no effect on the response curve (Figure 4.16). Regarding the cell density parameter, ρ , (Figure 4.21) high values lead to smaller tumors, but no

Table 4.2: List of parameters values (min, init and max) used for the parametric sensitivity analysis, together with the corresponding TCD₅₀ values obtained. The uncertainty (for a 95% level of confidence) of the calculated TCD₅₀ value is shown, only for the one corresponding to the initial parameter value. Parameter value variation in percentage is also shown for each parameter.

Symbol	Parameter value			Mean % variation	TCD ₅₀ (Gy)		
	min	init	max		min	init	max
DT_p	1.32	1.4	1.49	6	61.48	59.70 (± 1.09)	58.05
γ_{0h}	0.02	0.20	0.55	132	59.31		59.88
γ_1	5.0e-4	5.0e-3	31.8.0e-3	313	59.94		56.73
C_h	0.1	1	10	495	58.91		58.75
R	2.10	2.4	2.70	12.5	61.31		58.27
M_{th}	1.85	2	2.20	8.7	61.37		57.65
C_0	6.61e-7	6.61e-06	19.00e-6	138	57.94		63.77
C_1	4.51e-2	4.62e-2	4.72e-2	2.3	57.30		61.24
η_1	1.92e-7	1.96e-07	2.00e-7	2	61.24		56.73
η_2	1.7e-8	1.7e-07	1.7e-6	495	60.15		58.97
λ	4.59	4.69	4.81	2.3	61.76		56.85
a	3.04e-6	3.11e-06	3.18e-6	2.3	57.65		61.25
ϵ_ξ	3.08	3.17	3.25	2.6	57.42		61.20
ϵ_δ	0.07	0.7	7.00	495	58.79		59.53
ρ	0.89e8	1e8	1.13e8	12	58.79		60.16

significant difference in the TCD₅₀ value is observed. Finally, the parameters standing for the healthy cells growth rate, γ_{0h} , the necrotic cells ground elimination, ϵ_δ , and the healthy tissue apoptosis rate factor, C_h , (Figures 4.8, 4.20 and 4.10) showed to have no effect on the tumor evolution and response, in the ranges studied.

The parameters values (min, init and max) used for the parametric sensitivity analysis, and the corresponding values of TCD₅₀ resulted from the response simulations for each parameter value, are summarized in Table 4.2. The variation of the parameter value in percentage is also shown (column 5). This number corresponds to the average value of the percent variation in both directions.

5. Discussion

5.1 The tumor model

A model of tumor growth and tumor response to radiotherapy treatment was developed and studied. With the simulations performed it was verified that the model is able to adequately reflect well known tumor behaviors such as: initial exponential growth and proliferation saturation due to deprivation of nutrients and oxygen; tumor regression as a response to radiation, and the effect of hypoxia on the tumor response to treatment.

The model agrees within uncertainties with pretreatment experimental data of tumor growth and, in some cases, with radiation treatment tumor response data. Nevertheless, there is scarce bibliography to assure the clinical significance of the values associated in this thesis to some parameters. This study included the development of a tool to visually analyze how the model parameters affect tumor growth and response to treatment. In the following lines, a discussion about some relevant biological aspects related to certain model parameters or assumptions is presented.

5.1.1 Tumor composition: proportion of cancer and healthy cells

Solid tumors are complex structures composed of cancer (neoplastic) cells and stroma, in variable proportions. The stroma is the supportive tissue of neoplastic cells and comprises extracellular matrix components (e.g., proteins, collagen) and nonmalignant cells such as fibroblasts, blood vessels, inflammatory cells, macrophages, among others. Tumor cells can be classified in proliferating and non-proliferating cells [39]. Within the first ones, one can find: cancer stem cells, which have unlimited proliferative capacity, responsible for initiating and driving tumor growth, and finitely proliferating cells. The proportion of cancer and normal cells within a tumor is not clearly established. Previous published studies state that surrounding stroma (therefore, non-cancer cells) is reduced in squamous cell carcinomas [40] while other authors suggest that, for many tumor types, most of the cells that comprises the tumor volume are not malignant [41]. What is clear is that the actual composition of the tumor microenvironment is highly variable, with differences even seen in different areas of the same tumor [42].

In this study, the tumor cells (P) represent the totality of cancer cells: stem, proliferative, and non-proliferative cells. Hence, the parameters referring to their properties stand for an average of the individual parts. In view of the lack of clear information about the percentage of tumor and normal (healthy) cells composing a tumor, tumor growth was simulated from two distinct initial conditions scenarios: tumor composition of 90% tumor cells and 10% healthy cells, and the inverse proportion. It is worth to mention that a real human tumor might differ in composition from an encapsulated tumor (as the xenograft model simulated here), for which a higher amount of tumor cells would be expected. Therefore, the assumption of 90% of tumor cells composing the initial tumor is perhaps closer to this scenario.

5.1.2 Doubling time

The doubling time (DT) is defined as the amount of time required for a quantity to double its value. In this context, it could refer to the number of cells of a certain type, or to a tumor volume. The DT of human tumors shows variability for different kinds of cancer cells and tumors types [43], and also depends on whether they grow in human patients or have been transplanted into experimental animals [14]. The doubling time is known to be also dependent on factors such as tumor volume, nutrient concentration [44], or tumor location [45]. The DT value should depend on the measuring time, since DT increases with tumor volume [14, 46, 47, 48]. This is related with the growth saturation usually arising from the lack of nutrients/oxygen. Although no clear specification about the standard procedure for assessing this parameter was found, it appears that an usual method is to measure, either the number of cells or volume, during the exponential phase of the tumor growth [44, 48].

Previous studies have reported different values for the DT of the FaDu cell line, for models *in vitro* (e.g., 2.08 days [49], 1.2 – 2.8 days [15]), or *in vivo* (e.g., 2.6 days [50], 3-4 days [51], 4 days [30], 4.48 days [37], 4.5 [52]). The *in vivo* values are reported as volume doubling time, while the *in vitro* values, although not explicitly said, should refer to population doubling time since it is the tumor cell line what has been proliferating.

Equation (3.13) is commonly used to calculate the tumor cells growth rate, assuming the exponential growth regime. Since in this model the DT_p stands for the tumor cells, this parameter should take values closer to the *in vitro* published values. However, the whole reported DT range (1.2 – 4.5 days) was considered for the fitting and the sensitivity analysis. This is justified considering the uncertainty on tumor composition previously explained (Section 5.1.1) and by the fact that this parameter might vary between different conditions of inoculation and others above mentioned. Note that, with the exception of set A1, the fitted DT_p values resulted within the range of the *in vitro* reported values (see Table 4.1).

5.1.3 Cell density

The number of cells contained in 1 cm³ of tumor is not exactly established and therefore it has been let as a variable in this model. Commonly, a tumor reaching 1 cm³ of volume, corresponding approximately to 1 g of weight, is assumed to contain 10⁹ cells [14] although different numbers have been suggested by other studies. This variability is reflected in other computational tumor models such as [36], where 10⁸-10⁹ cells for a H&N tumor of this size is assumed. On the other hand, it has been suggested [38] that mostly in epithelial tumors a number of 10⁸ might be more realistic, and even more, for desmoplastic tumors cellularity might be 10⁷/cm³. According to this information and assuming that different cell types have different sizes, in the present study the cellular density of the virtual tumor is adjusted through the parameter ρ , which is allowed to vary between 10⁷ and 10⁹ cells per cm³. However, a ρ value of 10⁸ resulted from all cases of tumor growth fitting (since this value was taken as the initial guess).

5.2 Simulations

5.2.1 Growth curves fitting

The present model was able to fit experimental curves chosen for comparison in this study. Sets A1 and B1 differ, among others, in the DT_p value, which is smaller for set B1. This could mean that, despite initially there are only 10% of tumor cells, most of them may be fastly proliferating cancer stem cells.

The adjustment of the parameters for sets A2 and B2 was performed manually in order to change the minimum number of parameters values with respect to sets A1 and B1. Since the fitting of the second FaDu experimental data (from Yaromina *et al.* [30]) was made using only two experimental points (the initial volume and (t_y, V_y)), a free parameter optimization (with the least square difference minimization method) may lead to a set of parameter values with no biological meaning.

From sets 1 to sets 2, two or three parameters (DT_p and ϵ_ξ , or, C_0 , C_1 and a) were modified in order to adjust to the experimental point (t_y, V_y) from [30] (see Table 4.1). Although it is the same tumor cell line as in [29], 1 and 2 refer to different experimental settings (different animals, different tumor sizes, etc.), hence it seems reasonable to get parameters values that are slightly different. Other parameters could have been varied from sets 1 to sets 2, since several combinations of parameter values can be found to fit the experimental curves.

5.2.2 Tumor response to a radiotherapy treatment

5.2.2.1 Evolution during and after a radiotherapy treatment

The evolution of the virtual tumors under a radiotherapy treatment of 30 fractions was simulated. From Figure 4.5 it is observed that after the end of the treatment, the number of cells increases again if any cell, cancer or healthy, survives. This is in agreement with the definition of tumor control: killing of all tumor cells.

Regarding the tumor microenvironment variations, in Figure 4.5 it is also observed that, after the first treatment fraction, the nutrient and oxygen availability (M) increases rapidly, which is consistent with the known reoxygenation process after irradiation. This is related with the large fraction of cells dying after every treatment fraction, which produces a nutrients/oxygen consumption decrease, allowing this quantity to increase. In set A2 the increment of M is rapid and reaches a value approximately equal to 44% of the well oxygenated M value ($M_0 = 4$). In set B2 this increment is slower than in A2 but reaches a higher M value (53% of the well oxygenated M value) after 30 fractions. Although the process of reoxygenation is reproduced by the model, initial levels of M are not achieved, i.e., only partial nutrients/oxygen recovery is observed. This could

be explained by the fact that vascular cells are included as part of healthy cells in this model, and thus they die due to radiotherapy in the same way that normal tissue does. In reality, vascular cells are not sensitive to the radiation doses applied in standard treatments (with 2 Gy per fraction) [53]. Consequently, there is a permanent portion of vascular tissue that maintains certain level of nutrients and oxygen supply, which is not simulated by this model. One way to improve this issue would be to consider vascular cells as an independent (more radioresistant) population of cells.

5.2.2.2 TCP with and without oxygen effect

TCP curves were calculated for both cases with and without considering oxygen effect, for the two virtual tumors A2 and B2. For both sets a shift on the TCD_{50} values was observed in Figure 4.6. This is consistent with the fact that hypoxia results in an increased radioresistance of the cells, which was considered in the construction of the model (equations (3.15) - (3.17)). This shift has been previously reported in the studies (about different tumor types) by Moulder *et al.* [54], Baumann *et al.* [55], and Wang *et al.* [56], among others. From these references, it is also observed that the shift magnitude varies between approximately 3 to 20 Gy. In the present study the resulting shift magnitude was 15.45 Gy for set A2 and 41.21 Gy for set B2.

For set A2, the TCD_{50} value resulted within the range reported by Yaromina *et al.* [30], (56-68 Gy), when oxygen effect is accounted for (Figure 4.6, left). Set B2 showed higher values of TCD_{50} , leading to agreement with the TCD_{50} reported in [30] when the oxygen effect is not accounted for. However, when oxygen effect is considered, this value exceeded the range reported in [30] by approximately 35 Gy (Figure 4.6, right). One explanation for this could be that, despite of the lower proportion of tumor cells considered as the initial condition in set B2, the amount of tumor cells when the treatment starts is similar for both sets (accounting for more than the 99% of the cells), and the proliferation rate (γ_{0p}) is larger in set B2, due to the smaller value of the doubling time parameter for this set. Additionally, set B2 presents a higher recovery of M (thanks to the larger amount of healthy cells, compared to A2), which implies a higher availability of nutrients/oxygen for P cells to grow.

Additionally, from Figure 4.6 it is observed that the TCP shift between both oxygen sce-

narios is larger for set B2. This could be explained considering that, at the moment in which treatment begins, this set presents a larger amount of healthy cells. This implies a higher reoxygenation and nutrient supply (higher M level) and consequently a larger cell proliferation. Then, when the oxygen effect is considered, the reduced cell killing is combined with this fact, producing a total proliferation rate higher than the corresponding one when no oxygen effect is accounted for. Consequently, tumor control is reached later, and the shift of the response curves results larger for set B2. Initially, the reason for the larger shift of set B2 was thought to be related with the larger tumor cells proliferation rate (because of the smaller DTp). In order to verify this, a simulation for set A2, with a smaller DTp value (same as in set B2) was performed. As a result, no change on the magnitude of the shift was observed. Then, the shift amplification effect mentioned was attributed to the difference in the reoxygenation capacity between both sets.

The evolution of M and the radiosensitivity parameter of tumor cells, $\alpha_{p\text{ eff}}$, during treatment, as a function of dose, was also calculated. This is shown in Figures 5.1 and 5.2 of the current section. These curves were generated plotting the mean values of M and $\alpha_{p\text{ eff}}$, over the n simulations performed, at each dose level (same as used for the TCP calculation). Curves on the left correspond to set A2 while curves on the right correspond to set B2.

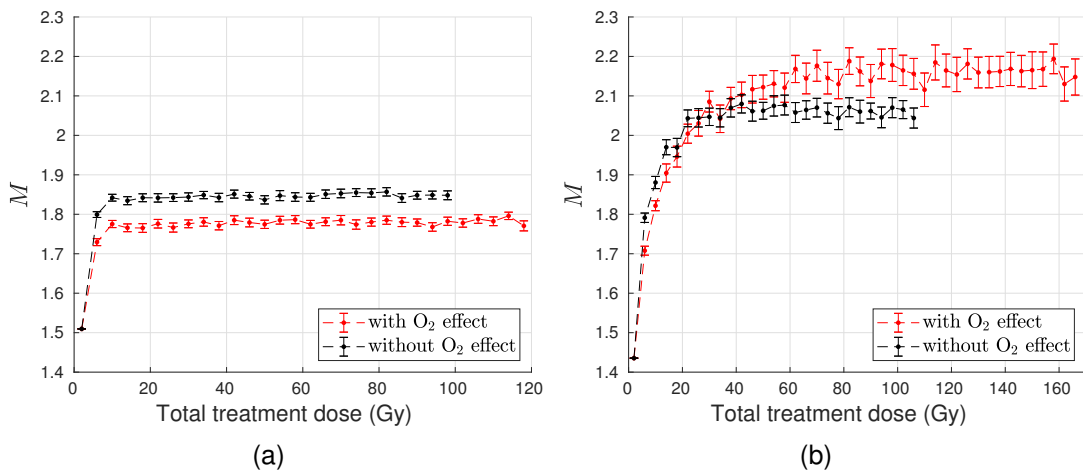


Figure 5.1: Evolution of nutrients/oxygen (M) (mean value over $n = 80$ simulations) as a function of the total treatment dose. Uncertainty bars corresponding to a 95% confidence interval are also included. (a) Set A2, (b) set B2.

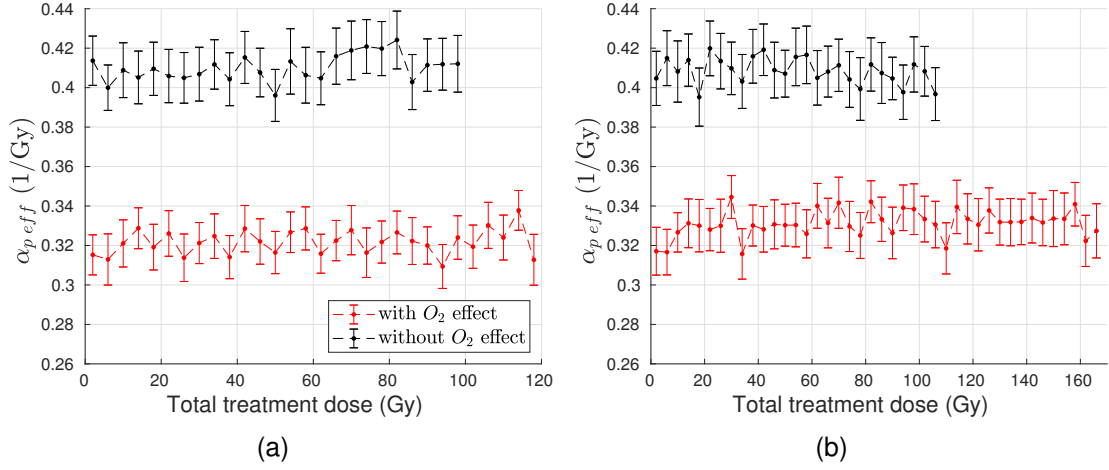


Figure 5.2: Evolution of radiosensitivity parameter for tumor cells ($\alpha_{p,eff}$) (mean value over $n = 80$ simulations) as a function of the total treatment dose. Uncertainty bars corresponding to a 95% confidence interval are also included. (a) Set A2, (b) set B2.

For set A2, it is observed that M takes higher values when no oxygen effect is considered. This is not observed in set B2, where M takes similar values for both curves at the beginning of the treatment, and later M becomes larger for the scenario considering the effect of oxygenation. The fact that M is higher when no oxygen effect is considered might be explained in the following way: when cell killing does not consider the oxygen effect, the α parameter is larger, leading to a larger cell killing. Consequently, after irradiation a smaller number of cells remains alive, causing a decreased consumption of nutrients/oxygen and finally leading to a larger M value. On the other hand, when the cell killing considers the presence of oxygen, i.e., the existence of hypoxia, the α parameter is lower, which results in less cell death (larger SF, see equation (3.15)). This implies more nutrients/oxygen consumption and consequently smaller values of M . This is observed in set A2 (less amount of healthy cells), where the evolution of M seems to be dominated by the cells consumption. Instead, in set B2 (higher amount of healthy cells than A2), the evolution of M is probably affected by the higher amount of healthy cells. Then, a higher healthy cell SF (i.e., considering oxygen effect) results in a higher availability of nutrients and oxygen (see equation (3.4)). This effect compensates the higher consumption, reason why the order of both curves results different for both sets.

Regarding the evolution of the radiosensitivity parameter α , from Figure 5.2, no important difference between A2 and B2 was observed. Additionally, for both sets, when

oxygen effect is considered, no obvious variability on the α value is appreciated during treatment. This is because the reoxygenation effect is not large enough to produce a variation on the α value distinguishable among the interpatient variability. This is verified in Figure 5.3, where the evolution of this quantity, for one patient, was plotted against dose. The α variation with respect its initial value (beginning of the treatment) is about 3% for set A2, and 7% for set B2. Therefore, this change is concealed when an interpatient variability of 15% is considered for the TCP calculation (in Figure 5.2).

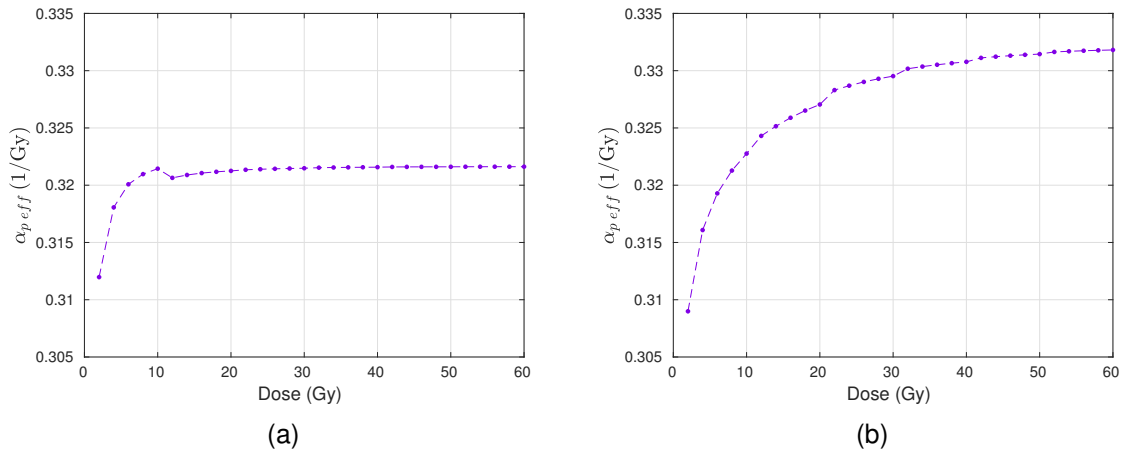


Figure 5.3: Evolution of radiosensitivity parameter for tumor cells ($\alpha_{p,eff}$) as a function of dose, for one patient. (a) Set A2, (b) set B2.

From this part of the study, it is also worth to note that for both cases, 90% and 10% of tumor cells composing the initial tumor, the percentage of tumor cells is more than 99% at the moment of the treatment. Moreover, despite the lower percentage of healthy cells at this time, the little difference existing between both sets on this quantity (0.02% versus 0.2%) implied a significant difference in the response. However, this observation should be taken with awareness of the given inter-relationship between the quantities M and H established by this model. This difference in response might suggest that when experimental studies of tumor control probability are performed, not only the tumor volume matters, but also the distribution of cells within the tumor at the moment of the treatment is relevant.

5.2.3 Parametric sensitivity analysis

A parametric sensitivity analysis of the present model was performed. This allowed to study the effect of the different parameters on tumor evolution and served to provide a consistency check of the tumor model developed in this work. For the majority of the parameters, the parameters value variation led to the expected results. In general, higher tumor growth rates were related to higher TCD_{50} values. For some other parameters, the interpretation of the resulting tumor growth and TCP curves was not straightforward. These ones are discussed in the following subsections. It is worth to note that, from the results displayed in Figures 4.7- 4.21, and according to the percent variation on the parameter value shown in Table 4.2, the parameters to which the model resulted to be more sensitive were: C_1 , η_1 , λ , a and ϵ_ξ (Figures 4.14, 4.15, 4.17, 4.18 and 4.19). These parameters were increased and decreased in a range of (2-2.7)%, which produced, on average, a variation of 3.4% on the TCD_{50} value.

5.2.3.1 Cell density ρ

A higher value of this parameter is observed to result in a smaller tumor volume growth rate. Nevertheless, this is only valid when the tumor volume is studied as a function of time. If, instead, the number of cells was analyzed, the behavior of the curves (cells versus time) for the min and max ρ values would be inverted, i.e., the higher density would result in a larger amount of cells within the tumor volume (data not shown). Despite the tumor growth curve changed with the variation of ρ (see Figure 4.21), practically no change is observed for the TCP curves (1.37 Gy of difference in TCD_{50}). This might be due to the fact that the difference in cell density is not large enough to modify the response. As it is pointed out by Webb and Nahum [57], as well as by Munro and Gilbert [58], the TCP varies slightly with the number of cells. More precisely, for a decrease of 1 order of magnitude in cell density, the ratio of the corresponding TCP values is about 1.69. The variation of ρ considered for this analysis was about 12% (mean value of the min and max value with respect the initial value). This implied a difference of 1.6% on the number of tumor cells at day 24 (when treatment starts), which resulted in a negligible difference on the TCD_{50} values.

5.2.3.2 Healthy cells consumption rate η_2

As shown in Table 4.2, η_2 was varied within a range of two orders of magnitude (which implied a mean percent variation of 495%). A small difference was observed in the tumor growth curves, between the minimum and maximum values, and no change in TCP was appreciated (Figure 4.16). However, the maximum value of this parameter, for which the corresponding growth curve is shifted with respect the other ones, exceeds the value of the consumption rate of tumor cells (by 1 order of magnitude). This would not in agreement with a real scenario, where tumor cells usually have a higher nutrients (such as glucose) consumption [59].

5.2.3.3 Parameters with negligible impact

The parameters γ_{0h} , corresponding to the growth rate of the healthy cells, C_h , standing for the healthy tissue apoptosis rate (compared to γ_1), and ϵ_δ , which accounts for the ground elimination of necrotic cells, turned out to have no effect on the growth and response curves in the range of values here examined (Figures 4.8, 4.10 and 4.20). Note that the parameter value variation was of more than 100% in the three cases. Therefore, the model might be simplified by fixing the value of these parameters. For example, the apoptosis rate could be the same for both type of cells, the healthy cell growth rate could be setted as half the value of the tumor cell growth rate, and the ϵ_δ parameter value could be fixed in some value within the range studied (for example, 0.5).

5.3 Limitations of this study

The model developed in this study helps to better understand tumor growth and response to radiotherapy, focusing on how different biological mechanisms are involved in tumor progression. However, as any mathematical model, there are limitations related with its implementation. These will be discussed in this section.

Some parameters included in this model have not been validated before. Consequently, it is a model containing some free parameters, which introduces a significant degree of degeneration. This implies that more than one combination of parameter

values allows to fit the experimental data of tumor growth and treatment response. Therefore, those values have to be carefully chosen from reasonable ranges based on biological information, which is currently limited.

Another limitation comes from the lack of consideration of the spatial dimension. The model only considers the overall status of the tumor size. Therefore, there is no information about the spatial distribution of tumor components, and no insight about how microscopic features of tumor composition and evolution are related with the macroscopic behavior.

This model considers that the tumor is composed by tumor and healthy cells, but it does not consider different kinds of subpopulations within the tumor cells. Additionally, there is uncertainty regarding the percentage of tumor and normal cells composing a tumor. This was only partially assessed comparing cases A and B in this study. Also, the model does not reproduce the complete reoxygenation process (i.e., recovery of nutrients/oxygen initial level) after irradiation, probably due to the fact that vascular cells are included within the healthy cells, therefore they die due to radiation as healthy tissue does.

The model is able to fit to available experimental data on tumor growth, and it also reproduces some experimental response data, finding agreement within uncertainties. However, no complete data sets, including growth and response for the same tumor, were found. Therefore, tumor growth and tumor response curves were compared with data of the same tumor type but from different studies. Only limited information about tumor growth was available for the response data set. A more correct validation of the model with experimental data would be possible if both sets of curves, from the same study, were available.

There are many biological mechanisms involved in tumor growth and response, a lot of them which are not completely understood today, such as the immune effect [60]. In a similar manner, clinical studies and data addressing these particular processes are still incomplete. Mathematical modeling is subject to the current understanding and therefore must make assumptions and simplifications of incompletely understood

biological processes.

6. Conclusion

A mathematical non-spatial model to simulate tumor growth and response to radiotherapy treatment was developed. A fitting to experimental tumor growth curves was performed in order to adjust the model parameters. The model is able to reproduce tumor behavior and to fit specific experimental data of tumor growth. In parallel, an open-source interface (coded in python), which allows to interactively study the impact of the different parameters in the tumor growth, was created. This tool might be specially useful as complementary material for radiobiology students as it helps to visualize the effect of different biological mechanisms in tumor growth.

Simulations of tumor response to radiotherapy were performed, with and without considering the effect of the oxygen on the cell killing. A shift on the TCP curves between both scenarios was verified. The response to treatment was found to be significantly sensitive to the amount of healthy cells within the tumor at the moment of irradiation. When oxygen effect was considered, the TCD_{50} value resulted within the range observed on the experimental data with which it was compared. The sensitivity of the model to the different parameters was also studied. In general, when the parameter variation implied higher tumor growth, higher TCD_{50} values were observed. The parameters C_1 , η_1 , λ , a and ϵ_ξ , were found to be the ones to which the model is more sensitive. The parameters γ_{0h} , C_h and ϵ_δ resulted to have negligible impact on the tumor growth and response.

The model developed was found to be significantly sensitive to the amount of healthy cells included in the tumor volume. The reoxygenation process after irradiation is however not completely reproduced by the model, probably because of the killing of vascular cells, considered as healthy cells.

The model developed allows to perform radiobiology studies and to compare results with different experimental data. It is a tool available for free use (the main code is included in the Appendix), versatile and easily editable to perform different simulations upon user requirement.

7. Future work

The developed model might be expanded to explore additional biological aspects and better reproduce tumor evolution.

The present model allows to easily change the treatment fraction size. Therefore, future studies exploring the outcome under other fractionation schedules can be performed. It would be also possible and interesting to study the response if the two cases of tumor composition considered in this study were defined at the moment when treatment starts, instead of being the tumor condition at time zero.

Regarding the model construction, it would be possible to simplify this model, for instance, by setting to constant values those parameters whose variation did not show great impact neither in tumor growth nor in response. This, in turn, would allow to better understand the behavior of the remaining parameters. At the same time, comparison of the model with more experimental data might be useful to identify the variability of the different parameters values between tumors, perhaps also allowing to fix certain model parameters values. Certainly, better knowledge about the mechanisms involved in tumor progression, allowing to establish more specific ranges of parameters values, is required in order to reduce the degree of degeneration of the model.

Another way to improve the present model might be to incorporate vascular cells as an independent quantity from healthy cells, therefore allowing to assign them a different radiosensitivity parameter. This could be significant for a better simulation of the process of reoxygenation after irradiation.

Finally, the incorporation of the spatial dimension into the model represents the largest future refinement with which the present model may be improved.

8. Bibliography

- [1] N. C. Institute, “What is cancer?” 2018. [Online]. Available: <https://www.cancer.gov/about-cancer/understanding/what-is-cancer>
- [2] Y. Lievens, M. Gospodarowicz, S. Grover *et al.*, “Global impact of radiotherapy in oncology: Saving one million lives by 2035,” *Radiotherapy and Oncology*, vol. 125, no. 2, pp. 175–177, 2017.
- [3] G. Delaney, S. Jacob, C. Featherstone, and M. Barton, “The role of radiotherapy in cancer treatment,” *Cancer*, vol. 104, no. 6, pp. 1129–1137, 2005.
- [4] D. Drasdo and S. Hoehme, “A single-cell-based model of tumor growth in vitro: monolayers and spheroids,” *Physical biology*, vol. 2, no. 3, p. 133, 2005.
- [5] C. Harting, P. Peschke, K. Borkenstein, and C. P. Karger, “Single-cell-based computer simulation of the oxygen-dependent tumour response to irradiation,” *Physics in Medicine and Biology*, vol. 52, no. 16, p. 4775, 2007.
- [6] I. Espinoza, P. Peschke, and C. Karger, “A voxel-based multiscale model to simulate the radiation response of hypoxic tumors,” *Medical physics*, vol. 42, no. 1, pp. 90–102, 2015.
- [7] R. A. Gatenby and E. T. Gawlinski, “A reaction-diffusion model of cancer invasion,” *Cancer research*, vol. 56, no. 24, pp. 5745–5753, 1996.
- [8] R. Wasserman, R. Acharya, C. Sibata, and K. Shin, “A patient-specific in vivo tumor model,” *Mathematical biosciences*, vol. 136, no. 2, pp. 111–140, 1996.
- [9] G. Lefebvre, F. Cornelis, P. Cumsille, T. Colin, C. Poignard, and O. Saut, “Spatial modelling of tumour drug resistance: the case of gist liver metastases,” *Mathematical medicine and biology: a journal of the IMA*, vol. 34, no. 2, pp. 151–176, 2016.
- [10] Y. Watanabe, E. L. Dahlman, K. Z. Leder, and S. K. Hui, “A mathematical model of tumor growth and its response to single irradiation,” *Theoretical Biology and Medical Modelling*, vol. 13, no. 1, p. 6, 2016.

-
- [11] M. Simeoni, P. Magni, C. Cammia *et al.*, “Predictive pharmacokinetic-pharmacodynamic modeling of tumor growth kinetics in xenograft models after administration of anticancer agents,” *Cancer research*, vol. 64, no. 3, pp. 1094–1101, 2004.
- [12] D. Bresch, T. Colin, E. Grenier, B. Ribba, and O. Saut, “Computational modeling of solid tumor growth: the avascular stage,” *SIAM Journal on Scientific Computing*, vol. 32, no. 4, pp. 2321–2344, 2010.
- [13] “Dictionary by merriam-webster: America’s most-trusted online dictionary.” [Online]. Available: <https://www.merriam-webster.com/>
- [14] M. C. Joiner and A. Van der Kogel, *Basic clinical radiobiology*. CRC press, 2016.
- [15] M. Molls, M. S. Anscher, C. Nieder, and P. Vaupel, *The impact of tumor biology on cancer treatment and multidisciplinary strategies*. Springer, 2009.
- [16] M. Morales, J. González, L. Bergues, A. Bergues *et al.*, “Is cancer a pure growth curve or does it follow a kinetics of dynamical structural transformation?” *BMC cancer*, vol. 17, no. 1, p. 174, 2017.
- [17] P. Cumsille, A. Coronel, C. Conca, C. Quiñinao, and C. Escudero, “Proposal of a hybrid approach for tumor progression and tumor-induced angiogenesis,” *Theoretical biology and medical modelling*, vol. 12, no. 1, p. 13, 2015.
- [18] E. Podgorsak, “Radiation oncology physics: a handbook for teachers and students,” *Br J Cancer*, vol. 98, p. 1020, 2008.
- [19] D. Ewing, “The oxygen fixation hypothesis: a reevaluation,” *American journal of clinical oncology*, vol. 21, no. 4, pp. 355–361, 1998.
- [20] B. G. Wouters and J. M. Brown, “Cells at intermediate oxygen levels can be more important than the “hypoxic fraction” in determining tumor response to fractionated radiotherapy,” *Radiation research*, vol. 147, no. 5, pp. 541–550, 1997.
- [21] P.-S. Tang, “On the rate of oxygen consumption by tissues and lower organisms as a function of oxygen tension,” *The Quarterly Review of Biology*, vol. 8, no. 3, pp. 260–274, 1933.

-
- [22] J. D. Chapman and A. E. Nahum, *Radiotherapy treatment planning: linear-quadratic radiobiology*. CRC Press, 2016.
- [23] A. E. Nahum, B. Movsas, E. M. Horwitz, C. C. Stobbe, and J. D. Chapman, "Incorporating clinical measurements of hypoxia into tumor local control modeling of prostate cancer: implications for the α/β ratio," *International Journal of Radiation Oncology• Biology• Physics*, vol. 57, no. 2, pp. 391–401, 2003.
- [24] V. Moiseenko, "Effect of heterogeneity in radiosensitivity on lq based isoeffect formalism for low α/β cancers," *Acta Oncologica*, vol. 43, no. 5, pp. 499–502, 2004.
- [25] I. El Naqa, J. Bradley, A. I. Blanco *et al.*, "Multivariable modeling of radiotherapy outcomes, including dose–volume and clinical factors," *International Journal of Radiation Oncology• Biology• Physics*, vol. 64, no. 4, pp. 1275–1286, 2006.
- [26] "Project jupyter," 2018. [Online]. Available: <http://jupyter.org/>
- [27] D. Sano, F. Matsumoto, D. R. Valdecanas *et al.*, "Vandetanib restores head and neck squamous cell carcinoma cells' sensitivity to cisplatin and radiation in vivo and in vitro," *Clinical Cancer Research*, vol. 17, no. 7, pp. 1815–1827, 2011.
- [28] A. Labs, "Fadu xenograft model." [Online]. Available: <http://altogenlabs.com/xenograft-models/other-bladder-cervical/fadu-xenograft-model/>
- [29] K. D. Bothwell, M. Folaron, and M. Seshadri, "Preclinical activity of the vascular disrupting agent oxi4503 against head and neck cancer," *Cancers*, vol. 8, no. 1, p. 11, 2016.
- [30] A. Yaromina, T. Kroeber, A. Meinzer *et al.*, "Exploratory study of the prognostic value of microenvironmental parameters during fractionated irradiation in human squamous cell carcinoma xenografts," *International Journal of Radiation Oncology• Biology• Physics*, vol. 80, no. 4, pp. 1205–1213, 2011.
- [31] L. Skarsgard and I. Harrison, "Dose dependence of the oxygen enhancement ratio (oer) in radiation inactivation of chinese hamster v79-171 cells," *Radiation research*, vol. 127, no. 3, pp. 243–247, 1991.

-
- [32] Å. Søvik, E. Malinen, Ø. S. Bruland, S. M. Bentzen, and D. R. Olsen, "Optimization of tumour control probability in hypoxic tumours by radiation dose redistribution: a modelling study," *Physics in Medicine & Biology*, vol. 52, no. 2, p. 499, 2006.
- [33] K. Pekkola-Heino, M. Jaakkola, J. Kulmala, and R. Grénman, "Comparison of cellular radiosensitivity between different localizations of head and neck squamous-cell carcinoma," *Journal of cancer research and clinical oncology*, vol. 121, no. 8, pp. 452–456, 1995.
- [34] M. Stuschke and H. D. Thames, "Fractionation sensitivities and dose-control relations of head and neck carcinomas: analysis of the randomized hyperfractionation trials," *Radiotherapy and oncology*, vol. 51, no. 2, pp. 113–121, 1999.
- [35] E. J. Hall, A. J. Giaccia *et al.*, *Radiobiology for the Radiologist*. Lippincott Williams & Wilkins Philadelphia:, 2006, vol. 6.
- [36] L. Marcu, T. Van Doorn, S. Zavgorodni, and I. Olver, "Growth of a virtual tumour using probabilistic methods of cell generation," *Australasian Physics & Engineering Sciences in Medicine*, vol. 25, no. 4, p. 155, 2002.
- [37] M. H. Starmans, D. Zips, B. G. Wouters *et al.*, "The use of a comprehensive tumour xenograft dataset to validate gene signatures relevant for radiation response," *Radiotherapy and Oncology*, vol. 92, no. 3, pp. 417–422, 2009.
- [38] U. Del Monte, "Does the cell number 10⁹ still really fit one gram of tumor tissue?" *Cell Cycle*, vol. 8, no. 3, pp. 505–506, 2009.
- [39] L. Marcu, E. Bezak, and B. Allen, *Biomedical physics in radiotherapy for cancer*. Csiro publishing, 2012.
- [40] M. Danciu, "Tumors (neoplasia)," 2009. [Online]. Available: <http://www.pathologyatlas.ro/tumors-neoplasia.php>
- [41] P. Mayles, A. E. Nahum, and J.-C. Rosenwald, *Handbook of radiotherapy physics: theory and practice*. CRC Press, 2007.
- [42] "Tumor-host interactions." [Online]. Available: <https://www.cancerquest.org/cancer-biology/tumor-host-interactions>

-
- [43] “Nci dictionary of cancer terms.” [Online]. Available: <https://www.cancer.gov/publications/dictionaries/cancer-terms/def/doubling-time>
- [44] C. J. Lin, J. R. Grandis, T. E. Carey *et al.*, “Head and neck squamous cell carcinoma cell lines: established models and rationale for selection,” *Head & neck*, vol. 29, no. 2, pp. 163–188, 2007.
- [45] J. C. Jansen, R. van den Berg, A. Kuiper *et al.*, “Estimation of growth rate in patients with head and neck paragangliomas influences the treatment proposal,” *Cancer*, vol. 88, no. 12, pp. 2811–2816, 2000.
- [46] U. Zätterström, A. Källén, and J. Wennerberg, “Cell cycle time, growth fraction and cell loss in xenografted head and neck cancer.” *In vivo (Athens, Greece)*, vol. 5, no. 2, pp. 137–142, 1991.
- [47] S. Benzekry, C. Lamont, A. Beheshti *et al.*, “Classical mathematical models for description and prediction of experimental tumor growth,” *PLoS computational biology*, vol. 10, no. 8, p. e1003800, 2014.
- [48] E. Mehrara, E. Forssell-Aronsson, H. Ahlman, and P. Bernhardt, “Specific growth rate versus doubling time for quantitative characterization of tumor growth rate,” *Cancer research*, vol. 67, no. 8, pp. 3970–3975, 2007.
- [49] S. Rangan, “A new human cell line (fadu) from a hypopharyngeal carcinoma,” *Cancer*, vol. 29, no. 1, pp. 117–121, 1972.
- [50] C. Petersen, W. Eicheler, H. Baisch *et al.*, “Impact of preirradiation of the tumour bed on cell production rate and cell loss of human fadu squamous cell carcinoma growing in nude mice,” *International journal of radiation biology*, vol. 75, no. 10, pp. 1293–1297, 1999.
- [51] C. Petersen, M. Baumann, H.-H. Dubben *et al.*, “Linear-quadratic analysis of tumour response to fractionated radiotherapy: a study on human squamous cell carcinoma xenografts,” *International journal of radiation biology*, vol. 73, no. 2, pp. 197–205, 1998.
- [52] A. Yaromina, D. Zips, H. D. Thames *et al.*, “Pimonidazole labelling and response to fractionated irradiation of five human squamous cell carcinoma (hsc) lines in

-
- nude mice: the need for a multivariate approach in biomarker studies,” *Radiotherapy and oncology*, vol. 81, no. 2, pp. 122–129, 2006.
- [53] H. J. Park, R. J. Griffin, S. Hui *et al.*, “Radiation-induced vascular damage in tumors: implications of vascular damage in ablative hypofractionated radiotherapy (sbrt and srs),” *Radiation research*, vol. 177, no. 3, pp. 311–327, 2012.
- [54] J. E. Moulder and S. Rockwell, “Hypoxic fractions of solid tumors: experimental techniques, methods of analysis, and a survey of existing data,” *International Journal of Radiation Oncology* Biology* Physics*, vol. 10, no. 5, pp. 695–712, 1984.
- [55] M. Baumann, S. Appold, J. Zimmer *et al.*, “Radiobiological hypoxia, oxygen tension, interstitial fluid pressure and relative viable tumour area in two human squamous cell carcinomas in nude mice during fractionated radiotherapy,” *Acta Oncologica*, vol. 40, no. 4, pp. 519–528, 2001.
- [56] J. Wang, X. Li, and N. Mayr, “Dose escalation to combat hypoxia in prostate cancer: a radiobiological study on clinical data,” *The British journal of radiology*, vol. 79, no. 947, pp. 905–911, 2006.
- [57] S. Webb and A. Nahum, “A model for calculating tumour control probability in radiotherapy including the effects of inhomogeneous distributions of dose and clonogenic cell density,” *Physics in Medicine & Biology*, vol. 38, no. 6, p. 653, 1993.
- [58] T. Munro and C. Gilbert, “The relation between tumour lethal doses and the radiosensitivity of tumour cells,” *The British journal of radiology*, vol. 34, no. 400, pp. 246–251, 1961.
- [59] R. Weinberg, *The biology of cancer*. Garland science, 2013.
- [60] M. Dougan and G. Dranoff, “The immune response to tumors,” *Current Protocols in Immunology*, pp. 20–11, 2009.

9. Appendix

9.1 Python interactive tool code

```
%matplotlib inline
import numpy as np
import pylab as plt
from ipywidgets import *
from scipy.integrate import odeint
from IPython.display import display

# Parameter initial values (d=days)
DTp = 2.0          # Doubling time tumor cells (d)
y0h = 0.2          # Proliferation rate healthy cells (1/d)
y1 = 5.0e-3        # Apoptosis rate tumor cells (1/d)
Ch = 1.0           # Apoptosis rate healthy cells (compared to y1)
R = 2.4            # Smoothing parameter
Mth = 2.0          # Hypoxia threshold
C0 = 6.61e-6       # Angiogenic capacity of healthy tissue (1/d)
C1 = 4.62e-2       # Link between nutrients/vascularization and EGFs (1/d)
eta1 = 1.96e-7     # Nutrient consumption rate by tumor cells (1/d)
eta2 = 1.70e-7     # Nutrient consumption rate by healthy cells (1/d)
lam = 4.7          # Elimination rate of angiogenic growth factor signal (1/d)
a = 3.11e-6        # Angiogenic excitability (1/d)
epsxi = 2.71       # Ground production of growth factor by cancer cells
epsdelta = 0.7     # Ground elimination of necrotic cells
rho_factor = 1.0   # Factor to change the cell density

# Definition of the function to simulate and plot tumor growth curve
def plot_evolution(R, Mth, DTp, y0h, y1, Ch, C0, C1, eta1, eta2, \
                  lam, a, epsxi, epsdelta, rho_factor):

    # Proliferation rate of tumor cells
    y0p = np.log(2)/DTp

    # Elimination rate of necrotic cells
    delta = np.log(2)/(7*(epsdelta+Mth))

    # Definition of growth and death rates functions for tumor cells
```

```

def ypp(M):
    if M <= 0:
        return 0
    else:
        return y0p*(1.+np.tanh(R*(M-Mth)))/2.

def ypd(M):
    E = -np.tanh(R*(M-Mth))
    if E>0:
        return y1*E
    else:
        return 0

# Definition of growth and death rates functions for healthy cells
def yhp(M,H):
    if M <= 0:
        return 0
    else:
        return y0h*(1.+np.tanh(R*(M-Mth)))/2.*(1-H/H0)

def yhd(M):
    E = -np.tanh(R*(M-Mth))
    if E>0:
        return Ch*y1*E
    else:
        return 0

# Definition of the rate of nutrient consumption for tumor cells
def eta_p(M):
    if M <= 0:
        return 0
    else:
        return eta1*np.tanh(M/Mth)

# Definition of the rate of nutrient consumption for healthy cells
def eta_h(M):
    if M <= 0:
        return 0
    else:
        return eta2*np.tanh(M/Mth)

```

```

# Initial conditons (Bothwell et al.)
P0 = rho_factor*0.90*67.77e5
H0 = rho_factor*0.10*67.77e5
N0 = 0.
M0 = 2.0*2
Xi0 = 2.

# Experimental data
time = [-1, 3, 5, 8, 11.0113, 14.0123, 17.0132, 20.0142]
volume = [67.7699, 227.738, 312.057, 370.37, 445.232, 643.814, 814.815, 758.865]
yneg = [44.9173, 122.143, 177.305, 202.522, 121.355, 11.8203, 159.18, 171.001]
ypos = [49.6454, 121.355, 178.881, 204.098, 123.719, 12.6084, 157.604, 173.365]
time_shift = 1 # for shifting the curve along the x axis
time = np.asarray(time)[:]+time_shift

# Define system of differential equations describing the tumor growth
def dW_dt(W, t):
    Wdot = np.zeros(5)
    Wdot[0] = (ypp(W[3]) - ypd(W[3]))*W[0] # Tumor cells
    Wdot[1] = (yhp(W[3], W[1]) - yhd(W[3]))*W[1] # Healthy cells
    Wdot[2] = ypd(W[3])*W[0] + yhd(W[3])*W[1] \
        - delta*(epsdelta+W[3])*W[2] # Necrotic cells
    Wdot[3] = C0*W[1]*(1. - W[3]/(2*Mth)) - eta_p(W[3])*W[0] \
        - eta_h(W[3])*W[1] + C1*W[4] # Nutrients/vascularization
    Wdot[4] = a*W[0]*(1. + epsxi - ypp(W[3])/(y0p+0.00001)) - lam*W[4] # EGF
    return Wdot

# Solve the ODE system
t = np.linspace(0, 40, 400)
W0 = [P0, H0, N0, M0, Xi0]
Wsol = odeint(dW_dt, W0, t)

# Store solution as volume values (mm^3)
P = Wsol[:, 0]*(1000/1e8)/rho_factor
H = Wsol[:, 1]*(1000/1e8)/rho_factor
N = Wsol[:, 2]*(1000/1e8)/rho_factor
M = Wsol[:, 3]
Xi = Wsol[:, 4]
# Define (simulated) tumor volume

```

```

tumor = (P + H + N)

# Plot simulated tumor growth curve together with the experimental growth curve
plt.plot(t, tumor, label="Tumor")
plt.errorbar(time, volume, yerr=[yneg, ypos], marker='o', \
             linestyle='-', color='k', capsize=5)
plt.plot(t, P, label="P")
plt.plot(t, H, label="H")
plt.plot(t, N, label="N")
plt.ticklabel_format(style='sci', axis='y', scilimits=(0,0))
plt.xlabel("Time_(days)")
plt.ylabel("Volume_(mm^3)")
plt.grid()
plt.legend()

# Define the slider buttons of each model parameter. Specification of the range
# of values, the step for varying the parameter value and the initial default
# parameter value.
R_slider = FloatSlider(min=0, max=15, step=0.1, value=R)
Mth_slider = FloatSlider(min=0.5, max=4, step=0.05, value=Mth)
DTp_slider = FloatSlider(min=0.5, max=5.5, step=0.01, value=DTp)
y0h_slider = FloatSlider(min=0, max=1.5, step=0.01, value=y0h)
y1_slider = FloatSlider(min=0, max=28, step=0.1, value=y1)
Ch_slider = FloatSlider(min=0.1, max=10, step=0.1, value=Ch)
C0_slider = FloatSlider(min=0, max=50, step=0.5, value=C0)
C1_slider = FloatSlider(min=0, max=8, step=0.01, value=C1)
eta1_slider = FloatSlider(min=0, max=4, step=0.01, value=eta1)
eta2_slider = FloatSlider(min=0, max=16, step=0.01, value=eta2)
lam_slider = FloatSlider(min=0, max=10, step=0.01, value=lam)
a_slider = FloatSlider(min=0, max=10, step=0.01, value=a)
epsxi_slider = FloatSlider(min=1, max=5, step=0.01, value=epsxi)
epsdelta_slider = FloatSlider(min=0, max=5, step=0.01, value=epsdelta)
rho_factor_slider = FloatSlider(min=0.1, max=10, step=0.01, value=rho_factor)

# Create interactive plot
interact(plot_evolution, R=R_slider, Mth=Mth_slider, DTp=DTp_slider, \
        y0h=y0h_slider, y1=y1_slider, Ch=Ch_slider, C0=C0_slider, C1=C1_slider, \
        eta1=eta1_slider, eta2=eta2_slider, lam=lam_slider, a=a_slider, \
        epsxi=epsxi_slider, epsdelta=epsdelta_slider, rho_factor=rho_factor_slider);

```

9.2 Matlab main codes

9.2.1 Tumor growth

```
% TUMOR GROWTH SIMULATION
% This function is called from another file which contains the parameter
% values and the initial conditions (IC) taken from the experimental data

function F = TumorGrowth(DTp, y0h, y1, Ch, R, Mth, C0, C1, ...
                        eta1, eta2, lambda, a, epsxi, ...
                        epsdelta, rho_factor, IC)

% FUNCTION INPUTS:
% y0p : Doubling time tumor cells (d=days)
% y0h : Proliferation rate healthy cells (1/d)
% y1 : Apoptosis rate tumor cells (1/d)
% Ch : Apoptosis rate healthy cells (compared to y1)
% R : Smoothing parameter
% Mth : Hypoxia threshold
% C0 : Angiogenic capacity of healthy tissue (1/d)
% C1 : Link between nutrients/vascularization and EGFs (1/d)
% eta1 : Nutrient consumption rate by tumor cells (1/d)
% eta2 : Nutrient consumption rate by healthy cells (1/d)
% lambda : Elimination rate of angiogenic growth factor signal (1/d)
% a : Angiogenic excitability (1/d)
% epsxi: Ground production of growth factor by cancer
% epsdelta: Ground elimination of necrotic cells
% rho_factor: Factor to change the cell density

% Initial conditions
P0 = IC(1)*rho_factor;
H0 = IC(2)*rho_factor;
IC = [P0;H0;IC(3);IC(4);IC(5)];

% Definition of rates of necrotic cells reabsorption and tumor cells growth
delta = log(2)/(7*(epsdelta+Mth));
y0p = log(2)/DTp;

% Definition of growth and death rates functions for tumor cells
function gamma_pp = ypp(M)
if (M<=0)
```

```

    gamma_pp = 0;
else
    gamma_pp = y0p*(1+tanh(R*(M-Mth)))/2;
end
end

function gamma_pd = ypd(M)
E = -tanh(R*(M-Mth));
if (E>0)
    gamma_pd = y1*E;
else
    gamma_pd = 0;
end
end

% Definition of growth and death rates functions for healthy cells
function gamma_hp = yhp(M,H,H0)
if (M<=0)
    gamma_hp = 0;
else
    gamma_hp = y0h*((1+tanh(R*(M-Mth)))/2)*(1-H/H0);
end
end

function gamma_hd = yhd(M)
E = -tanh(R*(M-Mth));
if (E>0)
    gamma_hd = Ch*y1*E;
else
    gamma_hd = 0;
end
end

% Definition of the rate of nutrient consumption for tumor cells
function Eta_p = eta_p(M)
if (M<=0)
    Eta_p = 0;
else
    Eta_p = eta1*tanh(M/Mth);
end
end

```

end

% Definition of the rate of nutrient consumption for healthy cells

function Eta_h = eta_h(M)

if (M<=0)

 Eta_h = 0;

else

 Eta_h = eta2*tanh(M/Mth);

end

end

% Definition of the System of ODEs describing tumor growth

function Wdot = f(t,W)

Wdot(1,1) = (ypp(W(4)) - ypd(W(4))) * W(1);

Wdot(2,1) = (yhp(W(4),W(2),H0) - yhd(W(4))) * W(2);

Wdot(3,1) = ypd(W(4)) * W(1) + yhd(W(4)) * W(2) - delta * (epsdelta + W(4)) * W(3);

Wdot(4,1) = C0 * W(2) * (1 - W(4) / (2 * Mth)) - eta_p(W(4)) * W(1) - eta_h(W(4)) * W(2) + C1 * W(5);

Wdot(5,1) = a * W(1) * (1 + epsxi - ypp(W(4)) / (y0p + 0.00001)) - lambda * W(5);

end

% Time step and time period for solving

increment = 0.01;

tspan = 0:increment:40;

% Solving the System of ODEs

[t,W] = **ode45**(@(t,W) f(t,W), tspan, IC);

% Store solution in new variables.

% Convert to volume values (mm³) for P, H and N cells.

P = W(:,1) * (1000/1e8) / rho_factor;

H = W(:,2) * (1000/1e8) / rho_factor;

N = W(:,3) * (1000/1e8) / rho_factor;

M = W(:,4);

Xi = W(:,5);

% Define tumor volume

tumor = P + H + N;

% FUNCTION OUTPUT

F = [t,P,H,N,M,Xi];

end

9.2.2 Tumor response to radiotherapy

% TUMOR GROWTH AND RADIOTHERAPY TREATMENT

*% This function is called from another file which contains the parameter
% values (of growth and response) and the initial conditions (IC) taken
% from the experimental data.*

```
function F = Growth_Radiotherapy(DTp, y0h, y1, Ch, R, Mth, C0, C1, eta1, eta2, ...  
                                lambda, a, epsxi, epsdelta, OERm, d, alpha_p, alpha_h, ...  
                                alphabeta_p, alphabeta_h, rho_factor, IC, OxygenEff)
```

% Initial conditions

```
P0 = IC(1)*rho_factor;  
H0 = IC(2)*rho_factor;  
IC = [P0;H0;IC(3);IC(4);IC(5)];
```

*% Definition of rate of necrotic cells reabsorption and rate of
% tumor cells growth*

```
delta = log(2)/(7*(epsdelta+Mth));  
y0p = log(2)/DTp;
```

% Determine if oxygen effect would be considered

```
if (OxygenEff==0)  
    km = 0;  
else  
    km = Mth*(OERm-2);  
end
```

% Definition of growth and death rates functions for tumor cells

```
function gamma_pp = ypp(M)  
if (M<=0)  
    gamma_pp = 0;  
else  
    gamma_pp = y0p*(1+tanh(R*(M-Mth)))/2;  
end  
end
```

```
function gamma_pd = ypd(M)  
E = -tanh(R*(M-Mth));  
if (E>0)
```

```

    gamma_pd = y1 * E;
else
    gamma_pd = 0;
end
end

% Definition of growth and death rates functions for healthy cells
function gamma_hp = yhp(M,H,H0)
if (M<=0)
    gamma_hp = 0;
else
    gamma_hp = y0h*((1+tanh(R*(M-Mth)))/2)*(1-H/H0);
end
end

function gamma_hd = yhd(M)
E = -tanh(R*(M-Mth));
if (E>0)
    gamma_hd = Ch*y1 * E;
else
    gamma_hd = 0;
end
end

% Definition of the rate of nutrient consumption for tumor cells
function Eta_p = eta_p(M)
if (M<=0)
    Eta_p = 0;
else
    Eta_p = eta1*tanh(M/Mth);
end
end

% Definition of the rate of nutrient consumption for healthy cells
function Eta_h = eta_h(M)
if (M<=0)
    Eta_h = 0;
else
    Eta_h = eta2*tanh(M/Mth);
end
end

```

end

% Definition of the OER as a function of M

```
function OER_value = OER(M)
OER_value = (M*OERm+km)/(M+km);
end
```

% Definition of the Alpha parameter as a function of M

```
function alpha_eff = Alpha(M, alpha)
alpha_eff = alpha*OER(M)/OERm;
end
```

% Definition of the AlphaBeta parameter as a function of M

```
function alphabeta_eff = AlphaBeta(M, alphabeta)
alphabeta_eff = alphabeta*OERm/OER(M);
end
```

% Definition of survival fraction of the LQ model

```
function sf = S(M, alpha, alphabeta)
sf = exp(-Alpha(M, alpha)*(d+d*d/(AlphaBeta(M, alphabeta))));
end
```

*% Definition of the System of ODEs, describing tumor growth before radiotherapy
% treatment and between treatment fractions of irradiation.*

```
function Wdot = f(t,W)
Wdot(1,1) = (ypp(W(4))-ypd(W(4)))*W(1);
Wdot(2,1) = (yhp(W(4),W(2),H0)-yhd(W(4)))*W(2);
Wdot(3,1) = ypd(W(4))*W(1) + yhd(W(4))*W(2) - delta*(epsdelta+W(4))*W(3);
Wdot(4,1) = C0*W(2)*(1-W(4)/(2*Mth))-eta_p(W(4))*W(1)-eta_h(W(4))*W(2)+C1*W(5);
Wdot(5,1) = a*W(1)*(1+epsxi-ypp(W(4))/(y0p+0.00001))-lambda*W(5);
end
```

% RADIOTHERAPY TREATMENT IMPLEMENTATION

% Time step and time period for solving

```
increment = 0.1;
tspan = 0:increment:140;
W = [];
t = [];
index_inf = 1;
current_fraction = 0;
```

```

dose_level = 0;
count_days = 0;

% Radiotherapy starts at day 24. 30 of 2 Gy are delivered (in this example),
% with no treatment during "weekends".
for i = 240:641
    if (mod(tspan(1,i),1)==0 && tspan(1,i)~=0)
        count_days = count_days+1;
        if ( mod(count_days+1,7) ~=0 && mod(count_days,7)~=0 )
            current_fraction = current_fraction+1;
            tspan_aux = tspan(1,index_inf:i);
            [t_aux,W_aux] = ode45(@(t,W) f(t,W), tspan_aux, IC);
            t = [t;t_aux];
            W = [W;W_aux];
            % Cell killing
            N_p = round(W(i,1));
            N_h = round(W(i,2));
            Sp = S(W(i,4),alpha_p, alphabeta_p);
            Sh = S(W(i,4),alpha_h, alphabeta_h);
            vec_randoms = rand(1,N_p);
            % Computation of living and death cells after treatment fraction
            P_alive = length(find(vec_randoms<=Sp));
            P_dead = length(find(vec_randoms>Sp));
            vec_randoms = rand(1,N_h);
            H_alive = length(find(vec_randoms<=Sh));
            H_dead = length(find(vec_randoms>Sh));
            % Update the initial conditions for solving the ODE system
            P0 = P_alive;
            H00 = H_alive;
            N0 = W(i,3) + P_dead + H_dead;
            M0 = W(i,4);
            Xi0 = W(i,5);
            IC = [P0;H00;N0;M0;Xi0];
            % Update the current dose level
            index_inf = i+1;
            dose_level = current_fraction*2;
        end
    end
end
end

```

```

% To compute evolution after treatment ends
tspan_aux2 = tspan(1,index_inf:size(tspan,2));
[t_aux,W_aux] = ode45(@(t,W) f(t,W), tspan_aux2, IC);
t = [t;t_aux];
W = [W;W_aux];

% Store solution. Convert to volume values (mm^3) for P, H and N cells.
P = W(:,1)*(1000/1e8)/rho_factor;
H = W(:,2)*(1000/1e8)/rho_factor;
N = W(:,3)*(1000/1e8)/rho_factor;
M = W(:,4);
Xi = W(:,5);
% Definition of tumor volume
tumor = P + H + N;

% Function OUTPUT
F = [t,tumor,P,H,N,M,Xi];
end

```

9.2.3 TCP simulation

```

% TCP SIMULATION
% This function is called from another file which contains the values of the growth
% parameters to be used, the initial conditions, the number of patients (NumOfRuns)
% to be simulated, and the value of the boolean 'OxygenEff' which tells whether the
% oxygen effect must be considered or not.

function [TCPcurve] = TCP(DTp, y0h, y1, Ch, R, Mth, C0, C1, eta1, eta2, lambda,...
    a, epsxi, epsdelta, rho_factor, IC, OxygenEff, NumOfRuns)

% Initial conditions
P0 = IC(1)*rho_factor;
H0 = IC(2)*rho_factor;
IC = [P0;H0;IC(3);IC(4);IC(5)];

% Definition of rate of necrotic cells reabsorption and rate of
% tumor cells growth
delta = log(2)/(7*(epsdelta+Mth));
y0p = log(2)/DTp;

```

```

% Radiotherapy parameters
OERm = 2.5;          % OER maximum value
d = 2;              % Fraction size
alpha_p = 0.41;     % Alpha for tumor cells
alpha_h = 0.13;     % Alpha for healthy cells
alphabetap = 10;    % Alpha/Beta for tumor cells
alphabetah = 4.4;   % Alpha/Beta for healthy cells

% Parameters for TCP calculation
mean_alpha = alpha_p; % Mean alpha value for the
                    % gaussian distribution
sigma_alpha = 0.15*alpha_p; % Sigma value for the gaussian
                    % distribution
N = NumOfRuns;      % Number of patients simulated

tcp = 0;
saturation = 0;
TCP_curve = [];
fraction = 1;
index = 1;

% TCP calculation
while (saturation < 7)
    dose_level = 2*fraction;
    n_control = 0;
    for i=1:N
        % Sort alpha value (of tumor cells) from a gaussian distribution
        sort_alpha_p = mean_alpha + sigma_alpha.*randn(1,1);
        % Call "Evolution". This function (almost equal to
        % "Growth_Radiotherapy") simulate tumor evolution under
        % radiotherapy treatment and stop the treatment when the
        % dose level desired is reached.
        % Ns : number of tumor cells alive after treatment
        Ns = Evolution(y0p, y0h, y1, Ch, R, Mth, delta, C0, C1, eta1, ...
                        eta2, lambda, a, epsxi, epsdelta, OERm, d, ...
                        sort_alpha_p, alpha_h, alphabetap, alphabetah, ...
                        IC, dose_level, OxygenEff);
        if (Ns==0)
            n_control = n_control+1;

```

```
        end
    end
    % Compute the tcp as the number of controlled cases over the total
    % number of patients simulated
    tcp = n_control/N;
    % Create the TCP curve
    TCP_curve(index,1) = dose_level;
    TCP_curve(index,2) = tcp;
    if (tcp==1), saturation=saturation+1; end
    fraction = fraction+2;
    index = index+1;
end

TCPcurve = TCP_curve;
end
```

Acknowledgements

First of all, I would like to sincerely thank to my main supervisors from Chile, Dr. Araceli Gago, Dr. Paola Caprile, and Dr. Ignacio Espinoza, who have guided my work very closely. Thank you for your availability, for every meeting and all the knowledge you have so generously shared with me. I feel very lucky of having had such a great team.

I would also like to thank my co-supervisor in Heidelberg, Dr. Christian Karger for his willingness to take part of this project. To Marcel Schaefer, program coordinator, for all the services provided and his enormous patience.

My gratitude also goes to Dr. Beatriz Sánchez, leader of the program in Chile, for the opportunity she gave me when she accepted me into the program, and her inspiring way to teach. Thanks to all the professors (from Chile and Germany) who took part of my learning during the master courses. And also thanks to the ones involved in my physics bachelor formation. Especially to Dr. Víctor Muñoz, from Universidad de Chile, undoubtedly one of the best professors I have met in my life, I will always thank his passion and his faith on me.

To my dear friends from the master, Rosario and Isabela. Because everything is so much easier with company. Thanks for all the words and the many hours spent studying together. Isa, this ending would have been so different without your help, I hope you know how grateful I am.

To my friends from life. In particular, I am happy to have reunited, just in time, with Catalina and Catalina. Thank you, girls, for appearing back in my life and for your understanding and support during this phase.

Last, but absolutely not least, I would like to thank to my family. To my dear sisters, Isidora and Domínica, and most especially to my parents, Iván and María Eugenia. Thanks for your infinite love and support. I could have never made it without you. Mamá, papá, esta tesis está dedicada a ustedes.